Stem Cell Reports
Article

OPEN ACCESS

A Subpopulation of Label-Retaining Cells of the Kidney Papilla Regenerates Injured Kidney Medullary Tubules

Juan A. Oliver,[1,*] Rosemary V. Sampogna,[1] Sumreen Jalal,[1] Qing-Yin Zhang,[2] Alexander Dahan,[1] Weiwei Wang,[1] Tian Huai Shen,[1] and Qais Al-Awqati[1,3,*]
[1]Department of Medicine
[2]Department of Pathology and Cell Biology
[3]Department of Physiology and Cellular Biophysics
Columbia University, New York, NY 10032, USA
*Correspondence: jao7@columbia.edu (J.A.O.), qa1@columbia.edu (Q.A.-A.)
http://dx.doi.org/10.1016/j.stemcr.2016.03.008

SUMMARY

To determine whether adult kidney papillary label-retaining cells (pLRCs) are specialized precursors, we analyzed their transcription profile. Among genes overexpressed in pLRCs, we selected candidate genes to perform qPCR and immunodetection of their encoded proteins. We found that *Zfyve27*, which encodes protrudin, identified a subpopulation of pLRCs. With *Zfyve27-CreERT2* transgenic and reporter mice we generated bitransgenic animals and performed cell-lineage analysis. Post tamoxifen, *Zfyve27-CreERT2* marked cells preferentially located in the upper part of the papilla. These cells were low cycling and did not generate progeny even after long-term observation, thus they did not appear to contribute to kidney homeostasis. However, after kidney injury, but only if severe, they activated a program of proliferation, migration, and morphogenesis generating multiple and long tubular segments. Remarkably these regenerated tubules were located preferentially in the kidney medulla, indicating that repair of injury in the kidney is regionally specified. These results suggest that different parts of the kidney have different progenitor cell pools.

INTRODUCTION

Epithelial organs such as the kidney appear to have a constant number of cells once they reach maturity. When cells die, adjacent terminally differentiated cells might divide within the plane of the epithelial sheet to replace them, but work in many organs indicates that often a more specialized pool of progenitor/stem cells exist to serve this function. To date, robust identification of progenitor/stem cells has required markers that are present in them but not in their surrounding cells and that, in addition, allow identification of their progeny. The function of many of these markers was largely unknown (at least initially); some had been cytoskeletal proteins; e.g., keratins (Rock et al., 2009), others were surface receptors such as LGR5 (Barker et al., 2007) or members of CD family, and many had nothing to do with "stemness." Yet, with genetic cell-lineage tracing they opened the way for the next leap in analytical power. Introduction of a genetic label under the control of the marker's promoter into the cells allowed identification of their in vivo location and, more significantly, permitted visualization of the contribution of single cells to multiple differentiated lineages in the same organ. Using this approach it was discovered that there appeared to be several stem cell pools in a given organ (Page et al., 2013; Donati and Watt, 2015); that there might be no obligatory hierarchy where a group of stem cells produced all differentiated subtypes during homeostasis (Sun et al., 2014), that there might be different stem cell pools that mediate homeostatic cell maintenance and organ regeneration (Tian et al., 2011; Mascré et al., 2012; Vaughan et al., 2015), and that injury can change lineage-restricted progenitor cells so that they become true stem cells (Ito et al., 2007; van Es et al., 2012).

The adult mammalian kidney is an organ with very low cell cycling during homeostasis but remarkable proliferating capacity after injury. It is still unresolved whether the kidney contains bona fide stem cells. Humphreys et al. (2008) genetically marked cells using *Six2*, a transcription factor expressed in embryonic kidney epithelial stem cells, and fate-mapped their progeny during adult kidney regeneration; they found that new epithelial cells after injury derived from cells of the same embryonic lineage. Although this study was interpreted to indicate that stochastic proliferation of terminally differentiated cells generates the new cells needed for kidney repair and that thus the adult kidney does not contain stem cells, it could not exclude that resident stem cell pools in the adult kidney might themselves be derived from the *Six2* compartment. During kidney regeneration from injury, Berger et al. (2014) performed cell-lineage analysis of a postulated proximal tubular epithelial stem cell population that was genetically labeled by doxycycline administration. When labeling was done before kidney injury (KI) the labeled cells did not expand, suggesting that these scattered proximal tubular cells were not stem/precursor cells. Similarly, labeling proximal tubular cells before injury followed by injury showed that there was no dilution of the label, which was interpreted as favoring the absence of a progenitor pool (Kusaba et al., 2014). Cell-lineage tracing has also been

applied to investigate the origin of podocytes, a particular target of many kidney diseases. Several lines of evidence suggested that adult podocytes might derive from the parietal epithelial cells lining Bowman's capsule (Ronconi et al., 2009), and Appel et al. (2009) found that a transgenic mouse with podocalyxin (expected to identify podocytes) unexpectedly expressed the transgene in the parietal epithelial cells. Inducible gene tagging of these cells with doxycycline showed that they generated podocytes but only in mice of young age, a time when kidney size increases dramatically. More recently, Rinkevich et al. (2014) used an unbiased approach to mark single-cell clones in the adult kidney and found that they generated long tubular segments along the nephron, strongly suggesting the presence of specialized progenitor cells that were segment specific in the nephron.

To search for stem cells in the adult kidney, we originally used the observation that many organ-specific stem cells cycle at very low rates, and with S-phase markers identified a population of low-cycling cells in the adult kidney papilla (Oliver et al., 2004, 2009). Since the cells retain these markers for long periods, we termed them papillary label-retaining cells (pLRCs). We found that following KI many of the pLRCs proliferated and occasionally located in other parts of the kidney, suggesting their involvement in organ regeneration. We thus postulated that the kidney papilla is a niche for progenitor/stem cells. However, as pLRCs divide, the S-phase label marking them dilutes into their daughter cells, and their identification has remained elusive. Genetic lineage tracing of the pLRCs would allow this, but a specific marker was lacking. To obtain such a marker, we isolated live pLRCs and appropriate control cells from the H2B-GFP mouse and analyzed their transcriptional profile. After selecting a small number of genes overexpressed in the pLRCs, we performed qPCR analysis of the candidate genes and immunolocalized their encoded proteins in the kidney. Among these, protrudin, a cytoplasmic protein encoded by *Zfyve27*, identified a population of pLRCs. We then used it to perform lineage analysis of these cells by generating *Zfyve27-CreERT2* transgenic mice. Our results show that in the adult kidney *Zfyve27-CreERT2*-marked cells preferentially located in the upper part of the papilla. These cells do not generate progeny during homeostasis and thus appear not to contribute to normal kidney maintenance. However, after KI, particularly if severe, these cells are activated and follow a complex program of proliferation, migration, and morphogenesis generating multiple and long tubular segments located preferentially in the kidney medulla, indicating a critical role in the repair of this region of the kidney. Our results thus suggest that different parts of the kidney have different progenitor cell pools.

RESULTS

Isolation of Live pLRCs and Transcriptome Analysis

To search for potential markers of pLRCs, we administered doxycycline to H2B-GFP mice during embryonic life and chased them for 2–3 months, at which time GFP$^+$ (i.e., LRCs) are essentially only found in the kidney papilla (Oliver et al., 2004, 2009). Single-cell suspensions of kidney papillae were subjected to fluorescence-activated cell sorting, and live GFP$^+$ cells (i.e., pLRCs) and GFP$^-$ control cells harvested for RNA extraction. In five independent experiments (each using both kidney papillae of nine H2B-GFP mice), mRNA from the live cells was amplified and analyzed by microarray. The results were deposited in the GEO website where they can be accessed (http://www.ncbi.nlm.nih.gov/geo/query/acc.cgi?acc=GSE71693). As detailed in Supplemental Experimental Procedures, 216 transcripts were consistently overexpressed by >5-fold in the pLRCs versus GFP$^-$ cells.

We confirmed the overexpression of the 30 highest-expressing genes in the GFP$^+$ versus GFP$^-$ cells using qPCR (Table S1). After consulting the databases of the Human Protein Atlas and Genepaint, we used antibodies for the proteins encoded by 19 of these genes (Table S2) and were able to detect 12 in the papilla. However, only one protein, protrudin (encoded by *Zfyve27*), located only in the papilla (and very rarely elsewhere in the kidney) (Figure 1A). In the H2B-GFP mouse, out of 1,008 GFP$^+$ cells 10% were positive for protrudin (Figure 1B), demonstrating that the cells expressing this protein are a subpopulation of pLRCs. Protrudin appeared to be a cytoplasmic protein similar to what was found previously (Shirane and Nakayama, 2006). There are only a few published studies on this protein, but it has been implicated in the control of vesicular traffic and neuronal protrusions (Shirane and Nakayama, 2006; Matsuzaki et al., 2011).

Zfyve27-CreERT2-Marked Cells in the Kidney

pLRCs are by definition low cycling, but they actively proliferate and generate new cells after KI (Oliver et al., 2004, 2009). However, proliferation of LRCs dilutes the retained S-phase label, preventing identification of their progeny. To perform genetic lineage-tracing analysis of pLRCs, we generated BAC transgenic *Zfyve27-CreERT2* mouse lines driven by the protrudin promoter. We mated these mice with Reporter-tdTomato (*R*-tdTomato) mice and generated bitransgenic *Zfyve27-CreERT2*;*R*-tdTomato mice. We examined their kidneys for the presence of spontaneous tdTomato-expressing cells in 2-week-old, 2-month-old, and 6-month-old mice (n = 3 at each age) and found no tdTomato$^+$ cells (not shown); thus, there was no Cre "leakage" in the absence of tamoxifen. In contrast, when *Zfyve27-CreERT2*;*R*-tdTomato adult mice were given

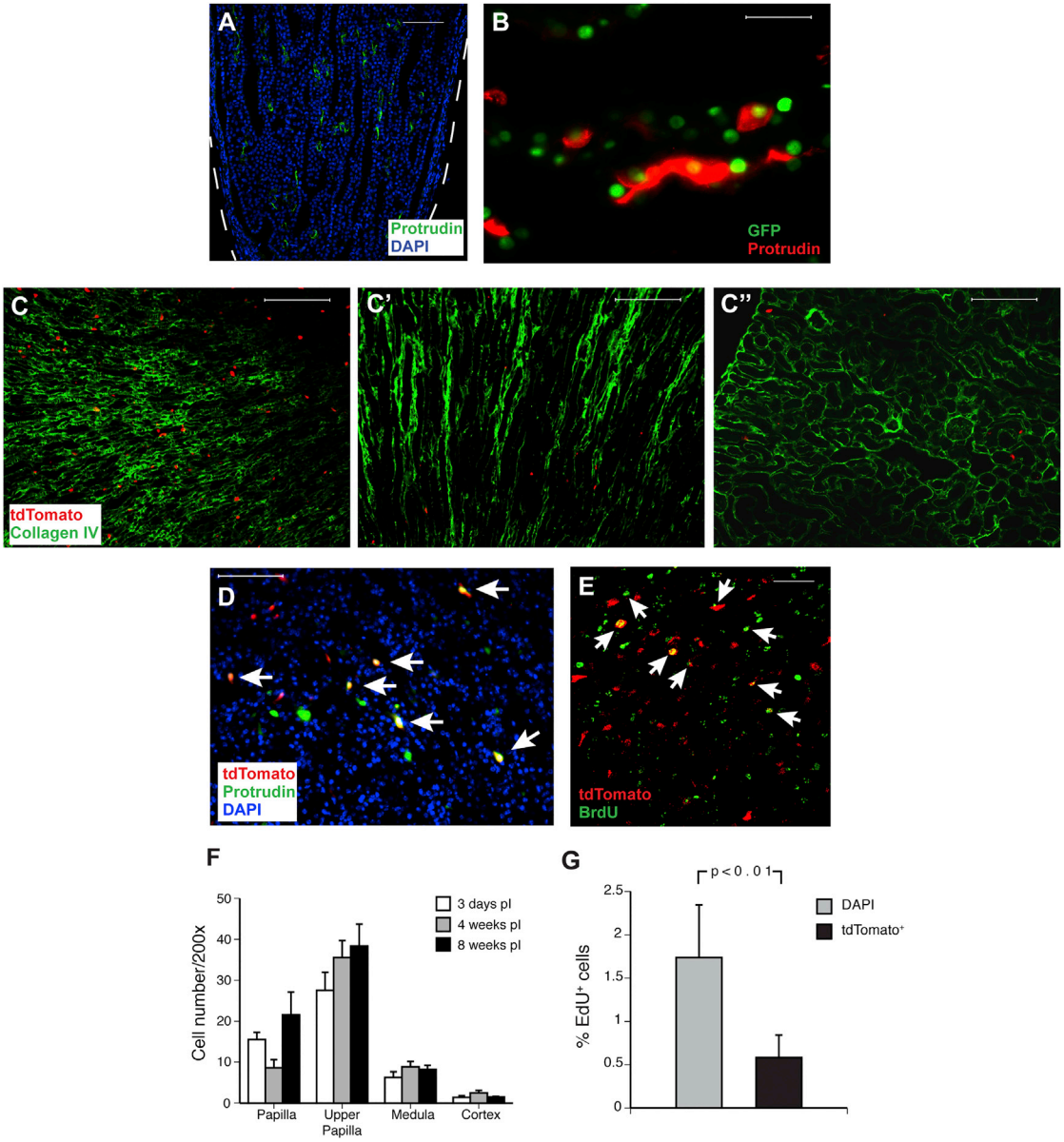

Figure 1. Kidney protrudin and *Zfyve27-CreERT2*-Marked Cells in Homeostasis

(A) Mouse kidney papilla with scattered cells positive for protrudin. The dashed line shows the edge of the papilla. Scale bar, 100 μm.

(B) Protrudin was detected in ~10% of pLRCs (n = 3 mice). Scale bar, 20 μm.

(C–C″) *Zfyve27-CreERT2*-marked cells in the upper papilla (C), medulla (C′), and cortex (C″) 2 weeks pTM. Scale bars, 100 μm.

(D) Protrudin was detected (arrows) in many of the *Zfyve27-CreERT2*-marked cells in the upper papilla 1 day pTM (n = 3 mice). Scale bar, 50 μm.

(E) About 8% of *Zfyve27-CreERT2*-marked cells in the papilla 3 days pTM were BrdU-retaining (arrows); i.e., pLRCs (n = 3 mice). Scale bar, 40 μm.

(F) *Zfyve27-CreERT2*-marked cells in different kidney regions 3 days (n = 10), 4 weeks (n = 6) and 8 weeks (n = 5) pTM. The number of cells did not significantly increase from those at 3 days pTM. Mean ± SE.

(G) The fraction of tdTomato$^-$ cells that incorporated EdU was significantly higher ($p < 0.01$) than that of the *Zfyve27-CreERT2*-marked cells. n = 3 mice 3 weeks pTM. Mean ± SE.

tamoxifen and examined 2 weeks post tamoxifen (pTM), a small population of scattered tdTomato$^+$ cells was detected in the kidney (see Figures 1C–1C″). Like pLRCs, *Zfyve27-CreERT2*-marked cells were most abundant in the upper part of the papilla (Figure 1C), which contained ~50% of all marked cells in the kidney while the rest of the papilla contained 33% of the cells. There were also scattered *Zfyve27-CreERT2*-marked cells in the medulla (13% of all labeled cells, Figure 1C′) and the cortex (4% of all labeled cells, Figure 1C″), albeit at much lower densities.

With immunofluorescence, protrudin was detected (Figure 1D, arrows) in 39% of 134 *Zfyve27-Cre*-marked cells in the upper papilla and papilla. In contrast, no *Zfyve27-Cre*-marked cells in the cortex and medulla were found to be positive for protrudin. Furthermore, of 576 bromodeoxyuridine (BrdU)-retaining papillary cells, 8% were tdTomato$^+$; i.e., marked by *Zfyve27-Cre*. Hence, *Zfyve27-CreERT2*-marked cells in the kidney papilla express protrudin and are a subpopulation of the pLRCs.

Like pLRCs (Oliver et al., 2004, 2009), the majority of *Zfyve27-CreERT2*-marked cells in the papilla appeared to be interstitial cells since they were present between collagen IV-positive basement membranes. However, also like pLRCs, a fraction of the *Zfyve27-CreERT2*-marked cells, averaging 25% (97 of 383 cells), were in collecting ducts (i.e., positive for AQP2; Figure S1A). Antibodies to AQP1 (identifying some thin descending limbs of Henle's loop) and to CLC-K1 (identifying thin ascending limbs) showed that few papillary *Zfyve27-CreERT2*-marked cells could be unambiguously located into these nephron segments, but the immunofluorescence signal of the thin segments of Henle's loop was weak. To obtain solid evidence for these structures, we used the more robust staining for protrudin in bitransgenic *Six2*-Cre;*R*-tdTomato mice (Humphreys et al., 2008) where epithelia of the papillary thin limbs of Henle's loop were easily identified by expressing tdTomato. We found (Figure S1B) that out of 4,269 tdTomato$^+$ cells in the papilla, 14% were positive for protrudin.

Thus, in the kidney papilla, protrudin is expressed in interstitial cells, collecting duct cells, and thin limbs of Henle's loop. In previous studies we located pLRCs in the interstitial and collecting duct cell compartments (Oliver et al., 2004, 2009) and when we now examined *Six2*Cre;*R*-tdTomato adult mice, we also found BrdU-retaining (i.e., pLRCs) cells in the thin limbs of Henle's loop of the papilla (see Figure S1C).

Additional analysis of the papillary *Zfyve27-CreERT2*-marked cells with antibodies giving a robust (i.e., control) signal showed that these cells were negative for CD140b and CD146 (markers of pericytes/mesenchymal stem cells), CD68 (macrophages), CD11c (dendritic cells), p75NGFR (neural crest-derived cells) and α-smooth muscle actin. Recently, a sparse population of kidney cells expressing *Sox9*$^+$ and generating progeny after injury was described in the kidney cortex and medulla (Kumar et al., 2015), but we found that *Zfyve27-CreERT2*-marked cells did not stain for *SOX9* in these regions. However, a small fraction of the *Zfyve27-CreERT2*-marked cells in the upper papilla (17%) were Sox9$^+$ (not shown). Finally, we characterized the papillary *Zfyve27-CreERT2*-marked cells using flow cytometry. We found (Table S3) that many tdTomato$^+$ were positive for the cell-surface markers CD24, CD133, ITGB1(CD29), and ITGA6(CD49f) as well as SCA1, CXCR4, and CXCR7, albeit, surprisingly, substantial numbers of all other papillary cells were also positive for these markers. As shown, cell selection by combining CXCR4 and CXCR7 expression provided the sharpest distinction between *Zfyve27-CreERT2*-marked and non-marked papillary cells.

In the medulla and cortex, most of the *Zfyve27-CreERT2*-marked cells were interstitial and did not express any segment-specific markers. There were very few cells that could be identified as intratubular epithelial cells and some of them did express segment-specific markers. Of 553 cells, 18 were inside collagen IV basement membranes, two of which were megalin$^+$, seven Tamm Horsfall protein$^+$ (THP), and two calbindin$^+$ (n = 6 mice). Thus, the marked cells were rarely present in differentiated epithelial structures and when there about half of them expressed the characteristic marker of that segment.

In summary, the *Zfyve27-CreERT2*-marked cells in the papilla are a subpopulation of pLRCs that express several markers, suggesting a role as progenitor cells in adult kidney.

Zfyve27-CreERT2-Marked Cells during Homeostasis

In many organs, precursor/stem cells generate new cells only during homeostasis or only after organ injury or, at least in principle, under both conditions. To determine whether *Zfyve27-CreERT2*-marked cells contributed to organ maintenance in homeostasis, we quantified the number of tdTomato$^+$ cells in all areas of the kidney at different times following administration of tamoxifen (Figure 1F); as shown, the number of marked cells did not significantly increase from 3 days to 8 weeks pTM in any of the kidney regions.

In *Zfyve27-CreERT2*;*R*-tdTomato-marked cells with tdTomato at clonal (Romagnani et al., 2015) or near clonal density (of 1,193 cells only ten were not present as single cells; see Table S4), we examined kidneys for the presence of possible tracing events (i.e., contiguous groups of >5 tdTomato$^+$ cells derived presumably from a single-cell clone) at different times after tamoxifen. No tracing events were found in mice (n = 6) up to 4 months pTM. In mice analyzed up to 9 months pTM, very rare tracing events of marked cells were detected in three mice (total n = 6),

particularly in the medulla (Figure S2A), where sometimes tubules made up of marked cells were found (Figure S2A′). Only very rarely were tracing events detected in the cortex, as shown in the example of Figure S2A″. No tracing events were seen in the papilla.

Since one possible reason for the absence of tracing events is the large volume of the kidney and its low proliferation rate, we increased the number of marked cells by injecting the same dose of tamoxifen for five consecutive days. This resulted in an ~3- to 4-fold increase in the number of *Zfyve27-CreERT2*-marked cells (Figure S2B) in all regions of the kidney, and again the upper papilla contained most cells (Figure S2C). However, similar to the findings with 1 day of tamoxifen administration, the number of marked cells did not increase when the time after the drug was prolonged to 6 months (Figure S2B). In addition, in mice examined 6–9 months pTM (n = 4), we found no noticeable increase in tracing events from that observed after 1-day tamoxifen, suggesting that the initial number of marked cells had little effect on the frequency of detectable tracing events.

While these findings suggest that in homeostasis *Zfyve27-CreERT2*-marked cells very rarely proliferate, cell cycling in the adult kidney is normally very low and the cycling frequency of the marked cells could be that expected of all kidney cells. To test this, we administered ethyldeoxyuridine (EdU) to *Zfyve27-CreERT2;R*-tdTomato mice for 2 weeks, and the number of EdU^+ cells that expressed tdTomato (i.e., *Zfyve27-CreERT2*-marked) or were only detected by nuclear DAPI was quantified. As shown in Figure 1G, 1.74% of tdTomato-negative ($tdTomato^-$) cells were positive for EdU while only 0.58% of the *Zfyve27-CreERT2*-marked cells (i.e., $tdTomato^+$) were positive ($p < 0.01$). Interestingly this difference was equally apparent in the kidney cortex, medulla, and papilla regions (not shown), indicating that the *Zfyve27-CreERT2*-marked cells in all regions of the kidney cycle less frequently than their neighboring cells, further confirming their relationship to pLRCs.

Thus, in the normal kidney *Zfyve27-CreERT2*-marked cells cycle at lower frequency than most kidney cells and lineage-tracing analysis indicates that, except for very rare occasions, they do not contribute to the homeostasis of the organ.

Response of *Zfyve27-CreERT2*-Marked Cells to Kidney Injury

Recent studies in skin, lung, and intestinal regeneration have shown that some stem cell pools proliferate in homoeostasis, while others proliferate in response to injury. Even more surprising is the recent demonstration that in response to severe injury, specific stem cell populations are activated which differ from those that proliferate after only mild injury (Tian et al., 2011; Vaughan et al., 2015; Chen et al., 2015; Tarlow et al., 2014). Stimulated by these studies, we examined the response of the *Zfyve27-CreERT2*-marked cells to graded KI by occluding the left renal artery for 10, 20, 30, and 40 min, and 8 days later tracing events were counted. In mice with KI due to 10 min or 20 min of artery occlusion (n = 3 for both times), no tracing events were detected 8 days after KI (not shown).

Following 30 min of ischemia, tracing events were easily detected in all injured kidneys, predominantly in the medulla. The tracing events consisted of many contiguous $tdTomato^+$ cells, when examined transversally with multiple cuts by confocal microscopy (Figures 2A and 2A′), or tubular segments only containing $tdTomato^+$ cells (Figure 2B). These results indicate repopulation of tubules by the $tdTomato^+$ cells during kidney regeneration; i.e., kidney repair launches a tubulogenesis program by *Zfyve27-CreERT2*-marked cells. Most of these tubules were found in the medulla, with some in the cortex and none in the papilla. However, while the tubules with $tdTomato^+$ cells were easily detected, they were isolated and their abundance was sparse (~1–3 detected per full sagittal kidney section), particularly in kidneys of mice treated with a single tamoxifen dose. However, in kidneys subjected to 40 min of renal artery occlusion we found a marked increase in the incidence of new tubules made up of *Zfyve27-CreERT2*-marked cells (see quantification below), particularly in the kidney medulla. Figure 2C shows the medulla of an injured kidney 8 days after KI while Figure 2C′ shows the medulla of the contralateral normal kidney. When examined longitudinally, the length of the tubules containing multiple contiguous $tdTomato^+$ cells varied from ~30 μm to more than 200 μm; a graphic analysis of the lengths of 253 tubules is shown in Figure 2D where the median length was 62 μm (n = 5 mice). Occasionally, some of the tubules were very long, as shown in the ~235-μm tubular segment in Figure 2D′. The tubules preferentially located in the lower part of the medulla, the region contiguous to the papilla that contains abundant thick segments of Henle's loop, as shown in Figure 2E.

In sum, after severe KI, *Zfyve27-CreERT2*-marked cells at clonal (or near clonal) density generated multiple tubular structures in the kidney medulla, suggesting that they are precursor cells involved in repair of this part of the kidney. Remarkably, only severe injury led to full activation of this pool of progenitor cells, similar to what was seen in the skin and lung (Vaughan et al., 2015; Chen et al., 2015).

Proliferation of *Zfyve27-CreERT2*-Marked Cells during Kidney Repair

The generation of tubular structures after renal artery occlusion by *Zfyve27-CreERT2*-marked cells indicates that

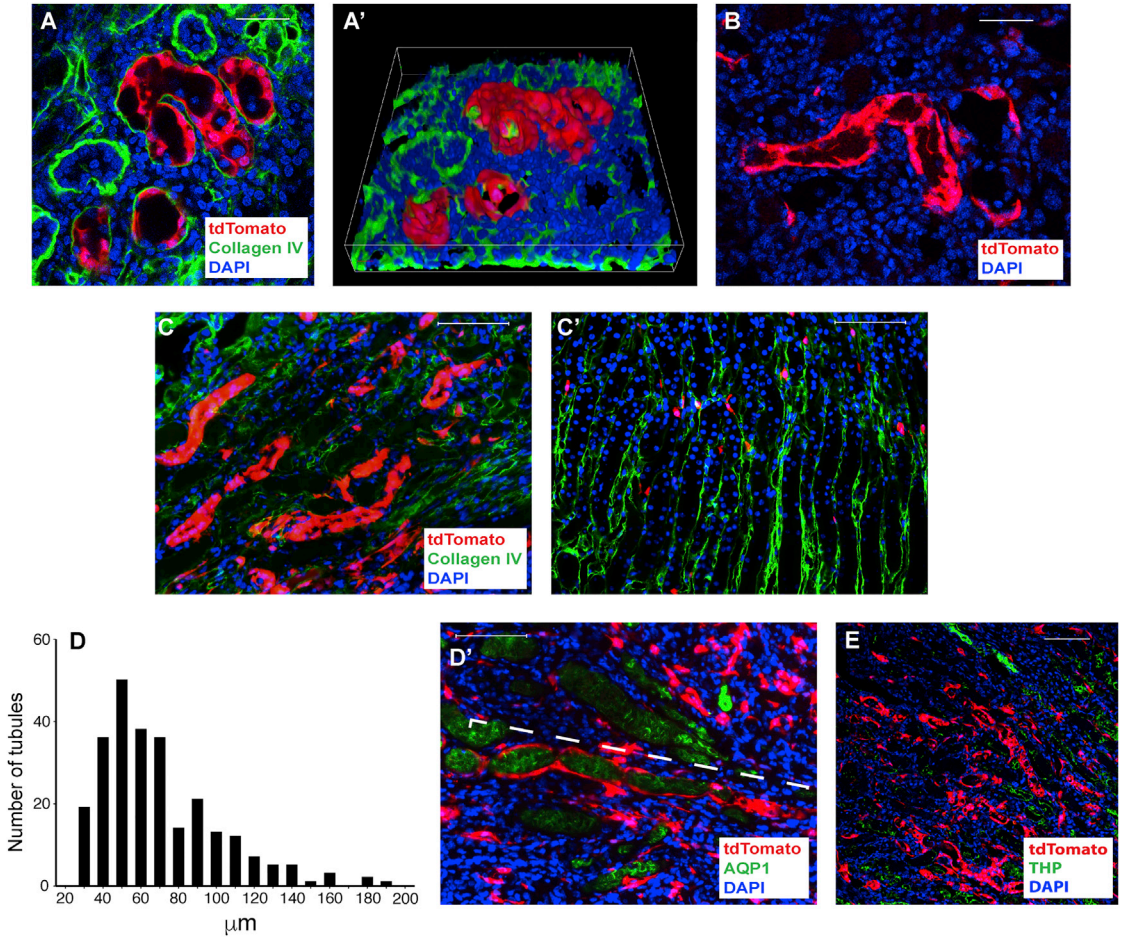

Figure 2. *Zfyve27-CreERT2*-Marked Cells during Kidney Repair from Injury

(A) Kidney medulla of mouse with 30 min KI 14 days pTM. Scale bar, 25 μm.

(A′) 0.3-μm confocal cut of kidney medulla with yz and xz stacks 5 days after KI.

(B) Kidney medulla of mouse with 30 min KI 3 days pTM. Longitudinal section of a medullary tubule made up of *Zfyve27-CreERT2*-marked cells 8 days after KI. Scale bar, 25 μm.

(C and C′) Kidney medullae of mouse subjected to 40 min KI 8 days pTM in the injured kidney (C) and contralateral non-injured kidney (C′) 8 days after KI. Scale bar, 50 μm.

(D) Bar graph of tubular length (μm) of 253 tubules measured in the kidney medulla 8 days after 40 min KI in mice 8 days pTM (n = 5 mice).

(D′) Long tubule of *Zfyve27-CreERT2*-marked cells (dashed white line = 235 μm) with a cast positive for AQP1 within it after 40 min KI 8 days pTM. Scale bar, 50 μm.

(E) The lower part of the medulla, with multiple thick ascending limbs of Henle's loop (positive for Tamm Horsfall Protein [THP]) contained the most tubules made by *Zfyve27-CreERT2*-marked cells; KI in mouse 8 days pTM. Scale bar, 100 μm.

the cells actively proliferate during kidney repair. However, the extensive apoptosis and necrosis caused by renal artery occlusion is followed by widespread proliferation of kidney cells that reaches its maximum 2–4 days post injury (Forbes et al., 2000). To examine whether *Zfyve27-CreERT2*-marked cells cycle similarly to other kidney cells, we induced renal artery occlusion to *Zfyve27-CreERT2*;*R*-tdTomato mice and administered EdU at 3, 8, and 21 days after KI and quantified the number of EdU$^+$ cell nuclei in both tdTomato$^+$ cells (i.e., *Zfyve27-CreERT2*-marked) and in cells solely identified by their DAPI nuclear staining (i.e., tdTomato$^-$ cells) in the injured kidneys.

As shown in Figure 3A and illustrated in Figure 3B, 3 days after KI, a time at which cellular proliferation is most marked (Forbes et al., 2000), a similar fraction of the tdTomato$^+$ and tdTomato$^-$ cells incorporated EdU (~15%), indicating that the *Zfyve27-CreERT2*-marked cells cycled as other kidney cells. However, at 8 days and 21 days after KI, cycling by the tdTomato$^-$ cells progressively declined while cycling by the tdTomato$^+$ cells

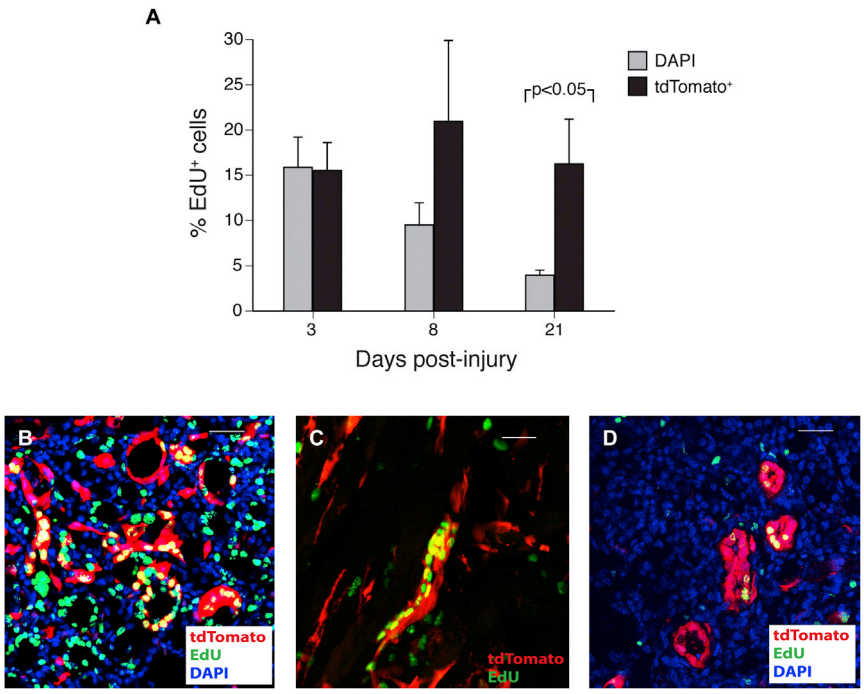

Figure 3. Proliferation of *Zfyve27-CreERT2*-Marked Cells during Kidney Repair from Injury

(A) Fraction (%) of tdTomato$^-$ cells (identified with DAPI) and of tdTomato$^+$ cells (i.e., *Zfyve27-CreERT2*-marked cells) that incorporated EdU at 3, 8, and 21 days after KI. EdU incorporation in tdTomato$^-$ cells 21 days after KI was significantly lower than at 3 and 8 days ($p < 0.05$) and, as shown in the figure, than that of the tdTomato$^+$ cells at this time ($p < 0.05$). n = 3–5 mice, 8 days pTM. Mean ± SE.

(B) EdU incorporation in the upper papilla of a *Zfyve27-CreERT2;R*-tdTomato mouse 3 days after KI. Scale bar, 40 μm.

(C) Cluster of tdTomato$^+$ cells in the upper papilla that incorporated EdU 8 days after KI. Scale bar, 40 μm.

(D) Tubules made up of tdTomato$^+$ cells that incorporated EdU 21 days after KI. Scale bar, 50 μm.

continued unabated (Figure 3A). At this time, we occasionally observed groups of proliferating tdTomato$^+$ cells in the upper papilla (Figure 3C), as we previously had seen with pLRCs in the H2B-GFP mouse (Oliver et al., 2009). As shown 21 days after KI in Figure 3A and illustrated in Figure 3D, proliferation by tdTomato$^+$ cells continued unchanged while cycling by tdTomato$^-$ cells had markedly decreased and approached, at this time, that of cells in normal kidneys (see Figure 1G). Indeed, the fraction of tdTomato$^-$ cells that incorporated EdU at 21 days after KI was significantly lower than at 3 ($p < 0.01$) and 8 days ($p < 0.05$) and that of the tdTomato$^+$ cells at this time ($p < 0.05$). Thus unlike unmarked cells, *Zfyve27-CreERT2*-marked cells have long-term proliferating potential.

Tubular Segments Regenerated from *Zfyve27-CreERT2*-Marked Cells Are Mostly in the Medulla

Tracing events generated from single-cell clones were recently described in the kidney during both homeostasis and after injury by Rinkevich et al. (2014), who used the ubiquitous actin promoter to conditionally activate Cre in the adult kidney of bitransgenic mice and randomly generated single-cell clones expressing a reporter protein. Long-term observation of normal kidneys or with KI revealed formation of nephron tubular segments made of clone-restricted cells. Since the tubules were restricted to specific nephron segments, these results suggested the presence of fate-restricted precursor cells in different parts of the nephron.

Thus, as with the actin-Cre construct, *Zfyve27-CreERT2* might have stochastically marked fate-restricted precursor cells and their proliferation after KI generated the new tubules made of *Zfyve27-CreERT2*-marked cells. To test this, we designed parallel experiments with mice that are likely to express tdTomato in kidney cells in a random manner. We used the *Rosa26-CrERT2* mouse, which in the *Rosa26* locus contains CreERT2, to generate bitransgenic *Rosa26-CrERT2;R*-tdTomato. For comparison of the response to KI of *Zfyve27-CreERT2;R*-tdTomato mice with that of the *Rosa26-CrERT2;R*-tdTomato, the number of tdTomato$^+$ cells had to be similar in both mouse lines, but administration of a low dose of tamoxifen (40 mg/kg) to *Rosa26-CrERT2;R*-tdTomato labeled all kidney cells (not shown). By progressively decreasing the tamoxifen dose to 5 mg/kg, as shown in Figure 4A, in *Rosa26-CrERT2;R*-tdTomato we marked comparable numbers of tdTomato$^+$ cells with those of *Zfyve27-CreERT2;R*-tdTomato mice. We then induced 40 min of left renal artery occlusion to both *Zfyve27-CreERT2;R*-tdTomato mice and *Rosa26-CrERT2;R*-tdTomato mice and harvested both the injured and contralateral, non-injured kidneys at 8 days after KI. Clonal analysis of the tdTomato cells present in the control kidney for both groups of mice (Figure S3B) showed that the vast majority of the cells were single clones (97% in *Zfyve27-CreERT2;R*-tdTomato and 93% in *Rosa26-CrERT2;R*-tdTomato mice). In contrast, the injured kidneys in both mouse strains showed multiple tubules that contained either ten or more contiguous marked cells when

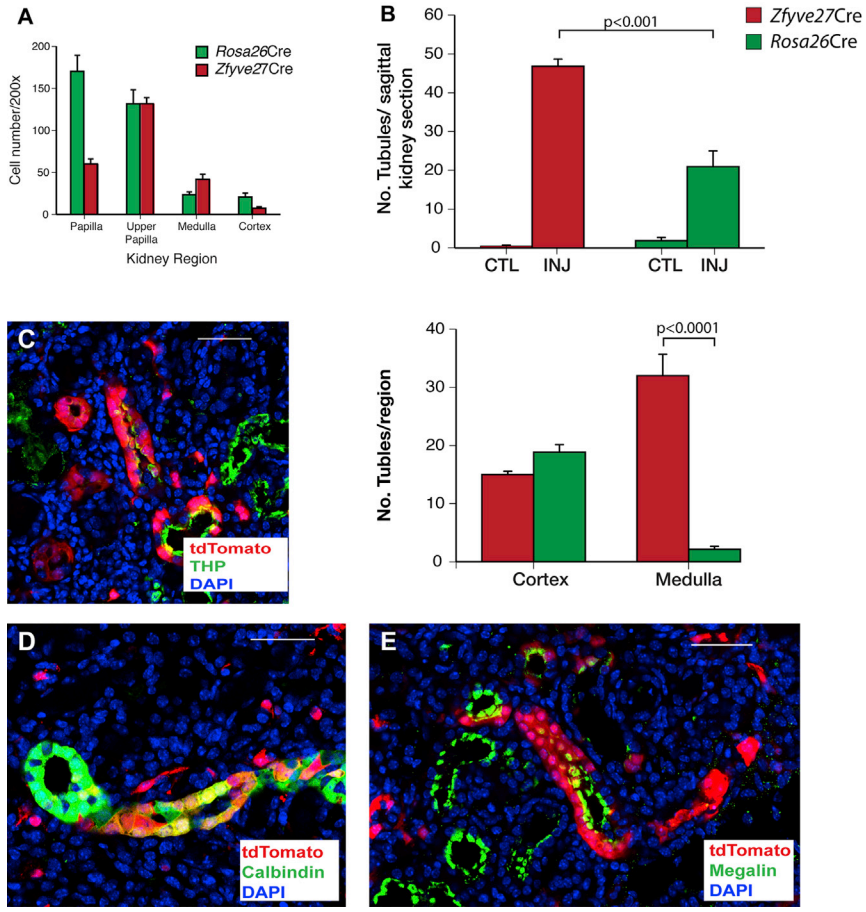

Figure 4. Specificity of the New Tubular Segments Generated by *Zfyve27-CreERT2*-Marked Cells during Kidney Repair

(A) Number of tdTomato$^+$ cells in *Zfyve27-CreERT2;R*-tdTomato (n = 8) and *Rosa26-CreERT2;R*-tdTomato (n = 7) mice 8 days pTM. In the upper papilla, medulla, and cortex both groups had similar cell numbers but in the rest of the papilla, *Rosa26-CreERT2;R*-tdTomato mice had a much greater number ($p < 0.001$). Mean ± SE.

(B) Tubules made up of tdTomato cells in injured kidneys (INJ) of *Zfyve27-CreERT2;R*-tdTomato mice (n = 5; in red) and *Rosa26-CreERT2;R*-tdTomato mice (n = 6; in green) 8 days after KI, performed 8 days pTM. The average number of tubules per kidney section is shown in the top. Since independently of injury tamoxifen occasionally generated tubules in *Rosa26-CreERT2;R*-tdTomato mice (Figure S3B′), quantification of the tubules in both the injured (INJ) and non-injured kidneys (CTL, control) is shown. In both mice, KI induced generation of tubules made up of tdTomato$^+$ cells ($p < 0.0001$ versus the control kidney) but the number of tubules in the injured kidney of the *Zfyve27-CreERT2;R*-tdTomato mice was significantly greater than that in the *Rosa26-CreERT2;R*-tdTomato mice ($p < 0.001$). Mean ± SE. The regional distribution of the tubules made up tdTomato$^+$ cells is shown in the bottom panel. In the cortex, the number of new tubules was very similar for both groups of mice. In contrast, while the medulla of the *Zfyve27-CreERT2;R*-tdTomato mice contained 68% of the total number of new kidney tubules, the medulla of the *Rosa26-CreERT2;R*-tdTomato mice had very few (12%). Mean ± SE.

(C) Tubular structures made up of *Zfyve27-CreERT2*-marked cells expressing Tamm Horsfall protein (THP). Scale bar, 50 μm.

(D) Tubular structure made up of *Zfyve27-CreERT2*-marked cells expressing calbindin. Scale bar, 40 μm.

(E) Tubular structures made up of *Zfyve27-CreERT2*-marked cells expressing megalin. Scale bar, 50 μm.

sectioned longitudinally or only tdTomato$^+$ if sectioned transversally; their numbers are shown in Figure 4B (top). There were twice as many tubules generated in the *Zfyve27-CreERT2* mice ($p < 0.01$) despite a similar abundance of tdTomato-marked cells before injury. More noteworthy however, was the strikingly different location of the new tubules made up of tdTomato$^+$ cells, as shown in the lower panel of Figure 4B. In *Rosa26-CrERT2;R*-tdTomato mice almost all marked tubules were found in the kidney cortex (88%) and a small number (12%) in the medulla. In contrast, in *Zfyve27-CreERT2;R*-tdTomato mice most of the tubules of tdTomato$^+$ cells were found in the medulla (68%) while the cortex contained 32%.

To exclude the possibility that ischemic KI might activate *Zfyve27* and that the presence of residual tamoxifen 8 days pTM could account for our findings, we performed KI in *Zfyve27-CreERT2;R*-tdTomato mice at 4 and 8 weeks pTM and examined their kidneys 8 days after KI. In mice 4 weeks pTM (n = 3), we found an average of 60 tubules per sagittal kidney section (76% of them located in the medulla) and in mice 8 weeks pTM (n = 4) we found 55 tubules per sagittal kidney section (69% of which located in the medulla), in agreement with the data of Figure 4B.

A simple model of the data from Figures 4A and 4B would predict that if all single labeled cells can generate a clone of cells after injury, it would be expected that the number of labeled tubules in the injured kidneys would be similar to that of labeled cells in control kidneys. Indeed, in the kidney cortex the number of labeled tubules was similar to the number of individual cells in both the *Rosa26-Cre* mice (21 cells in control kidneys and 19 tubules in injured kidneys) and *Zfyve27-Cre* mice (7 cells and 15 tubules). In the medulla, however, the control *Rosa26-Cre* mice

Table 1. Fraction of Tubules Made of tdTomato$^+$ Cells with Nephron-Segment-Specific Markers after KI in *Zfyve27-CreERT2;R*-tdTomato and *Rosa26-CreERT2;R*-tdTomato Mice

	8 Days after KI (%)		4 Weeks after KI (%)	
	Medulla	Cortex	Medulla	Cortex
Zyve27-CreERT2;R-tdTomato				
Megalin	0	30	0	28
THP	12	0	21	9
Calbindin	11	0	8	26
AQP2	0	5	0	0
Rosa26-CreERT2;R-tdTomato				
Megalin	0	45	0	80
THP	0	0	0	0.2
Calbindin	0	0	0	0
AQP2	0	0	0	3

KI was performed 8 days pTM. *Zyve27-CreERT2;R*-tdTomato mice n = 5 at 8 days and n = 6 at 4 weeks. *Rosa26-CreERT2;R*-tdTomato mice n = 6 at 8 days and n = 5 at 4 weeks.

had 23 cells while *Zfyve27-Cre* mice had 42 cells. Yet the number of labeled tubules in the injured kidney medulla of *Rosa26-Cre* mice was only 2, while that of the *Zfyve27-Cre* mice was 32. Thus it appears that in the medulla, single cells labeled by *Zfyve27-Cre* led to the appearance of tubules after injury while the randomly labeled *Rosa26-Cre* cells rarely did. This suggests that the *Zfyve27-CreERT2*-marked cells are specific precursors of cells needed for repair of the kidney medulla after severe KI.

Differentiation of the Progeny of *Zfyve27-CreERT2*-Marked Cells

To identify the progeny generated by *Zfyve27-CreERT2*-marked cells after KI, we used nephron segment-specific cell markers. We probed kidney sections with antibodies to megalin (proximal tubule), THP (thick ascending limb of the loop of Henle), calbindin (distal tubule), and AQP2 (collecting duct). Although the kidney medulla also contains abundant thin ascending and descending loops of Henle, using several antibodies these nephron segments could not be consistently identified after KI and were excluded from analysis.

Eight days after KI injury, we found that some medullary tubules made of *Zfyve27-CreERT2*-marked cells were positive for THP (see example in Figure 4C) or calbindin (see Figure 4D). However, for THP, of 66 tubules examined only 8 (12%; see Table 1) were positive, and of 57 examined for calbindin, only 6 (11%) were positive. No tubule in the medulla was positive for megalin or AQP2 and, thus, the majority of the tubules were unidentified. Four weeks after KI, the number of tdTomato$^+$ tubules in the medulla identified as thick ascending limbs of Henle's loop (i.e., THP positive) had increased (Table 1) to 21% (16 of 76), indicating that expression of THP lags behind tubulogenesis during kidney repair. The frequency of tubules made up of *Zfyve27-CreERT2*-marked cells that were positive for calbindin did not significantly change (8%; 5 of 59) at 4 weeks. Thus, even at this late date, the majority of the new medullary tubules made of *Zfyve27-CreERT2*-marked cells did not express the terminally differentiated markers of these segments.

Interestingly, even though no tubule was identified as a proximal tubule in the medulla, a third of tdTomato$^+$ tubules in the cortex (see Table 1) were positive for megalin (see example in Figure 4E), both at 8 days (31%; 17 of 54) and 4 weeks after KI (28%; 5 of 18), suggesting that *Zfyve27-CreERT2*-marked cells in the medulla and cortex generate different progeny. In addition, 4 weeks after KI injury, 9% (4 of 46) of the cortical tubules were positive for THP and 26% (6 of 23) were positive for calbindin. Thus, unlike the medulla, almost 70% of all cortical tubules made up of tdTomato$^+$ cells could be identified 4 weeks after KI, with one third being proximal tubules, another third distal tubules, and ~10% thick ascending loops of Henle.

In *Zyve27-CreERT2;R*-tdTomato mice in which KI was induced 4 weeks (n = 3) and 8 weeks (n = 4) pTM, similar results were found in both groups and the data were pooled. Eight days after KI, of an average of 15 cortical tubules per kidney sagittal section, 33% were positive for megalin and of an average of 42 medullary tubules, 6% were positive for THP and 14% for calbindin, results comparable with those of Table 1.

In marked distinction to the findings in *Zfyve27-CreERT2;R*-tdTomato mice, in the injured kidneys of the *Rosa26-CrERT2;*-tdTomato mice the medulla very rarely had tubules (see Figure 4B, bottom), and in none expressed differentiation markers that allowed the segments to be identified. Most of the new tubules made up of tdTomato$^+$ cells in these mice were restricted to the kidney cortex (Table 1) and 4 weeks after KI, 80% of them (24 of 30) were MEGALIN positive, identifying them as proximal tubules.

Thus, most cortical tubules after KI in *Rosa26-CrERT2;*-tdTomato mice rapidly acquired their differentiation markers. However, recovery from injury in the medulla of *Zfyve27-CreERT2;R*-tdTomato was much slower, with only a small fraction of thick ascending and distal tubules acquiring their differentiated status. A possible reason for this is that these marked cells continue to proliferate for long periods of time (Figure 3A) and it is well known that differentiation is suppressed during cell division.

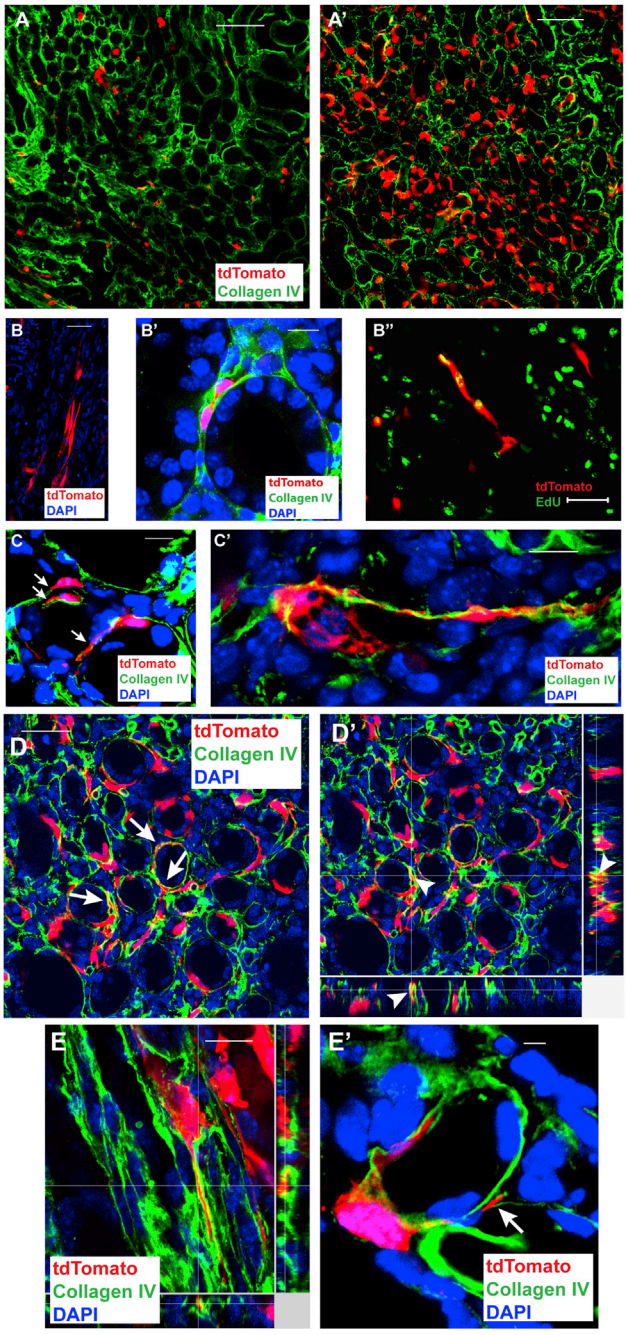

Figure 5. Migratory Phenotype of *Zfyve27-CreERT2*-Marked Cells during Kidney Repair

(A and A′) Transverse sections of the upper papillae in control (A) and injured (A′) kidneys of a *Zfyve27-CreERT2*;*R*-tdTomato mouse 3 days after KI, performed 10 days pTM. Scale bar, 40 μm.

(B–B″) High-power images of *Zfyve27-CreERT2*-marked cells with elongated bodies (B; scale bar, 30 μm), nuclear deformation (B′; scale bar, 20 μm), and association in chains (B″; scale bar, 25 μm).

(C and C′) The *Zfyve27-CreERT2*-marked cells displayed broad projections like lamellipodia (arrow in C) and finger-like projections typical of filopodia (C′). Both scale bars, 20 μm.

(D and D′) Transverse section of the kidney medulla 8 days after KI, performed 10 days pTM. Confocal 0.3-μm cut (D) and orthogonal projections (D′) showing that cell extensions penetrated collagen IV basement membranes (arrows in D and arrowheads in D′; scale bar, 50 μm).

(E) High-power confocal ortho-projection of a single *Zfyve27-CreERT2*-marked cell penetrating into the collagen IV matrix 8 days after KI performed 10 days pTM. Scale bar, 20 μm.

(E′) High-power confocal 0.3-μm cut of a single *Zfyve27-CreERT2*-marked cell with projections inside and outside (arrow) a tubule collagen IV basement membrane 8 days after KI performed 9 days pTM. Scale bar, 20 μm.

Migration of *Zfyve27-CreERT2*-Marked Cells after Kidney Injury

Repair of many epithelial organs involves, in addition to cell proliferation, a dynamic program of cell migration and differentiation (Blikslager et al., 2007; Veniaminova et al., 2013). Epithelial precursor cells actively migrate in *Drosophila* Malpighian tubules during homeostasis (Singh et al., 2007), and collective epithelial cell migration is an early response to injury in zebrafish kidney (Palmyre et al., 2014). Since we previously found that after KI some pLRCs migrated outside the kidney papilla (Oliver et al., 2009), we considered that since the majority of *Zfyve27-CreERT2*-marked cells were in the upper papilla, their migration toward the adjacent medulla could be the reason for preferential repair of these medullary nephron tubules.

In kidney sections of *Zfyve27-CreERT2*;*R*-tdTomato mice subjected to KI, we found that the *Zfyve27-CreERT2*-marked cells displayed multiple morphological characteristics of cell migration (Ridley et al., 2003). First of all, 3 days after injury, when compared with cells in the normal contralateral kidney, the tdTomato$^+$ cells in the upper papilla of the injured kidney broadened their shape and rounded around tubular structures (Figures 5A and 5A′). At higher power, many of these marked cells had elongated bodies (Figure 5B), narrow nuclei (Figure 5B′), and frequently aggregated in chain-like structures (Figure 5B″). In addition, as in regeneration in other epithelia, multiple cells had prominent cellular protrusions, either with the broad shape characteristic of lamellipodia (Figure 5C) or finger-like filopodia (Figure 5C′). None of these shape changes were seen in the uninjured contralateral kidney.

Remarkably, many of the tdTomato$^+$ cells were found to invade and traverse the collagen IV basement membranes, as shown in the confocal images of a transverse section of the kidney medulla (Figures 5D and 5D′). A high-power view of these cells revealed cellular protrusions that invaded the extracellular matrix (Figure 5E) or crossed the basement membrane of tubular structures (Figure 5E′). We suggest that the traversal of the basement

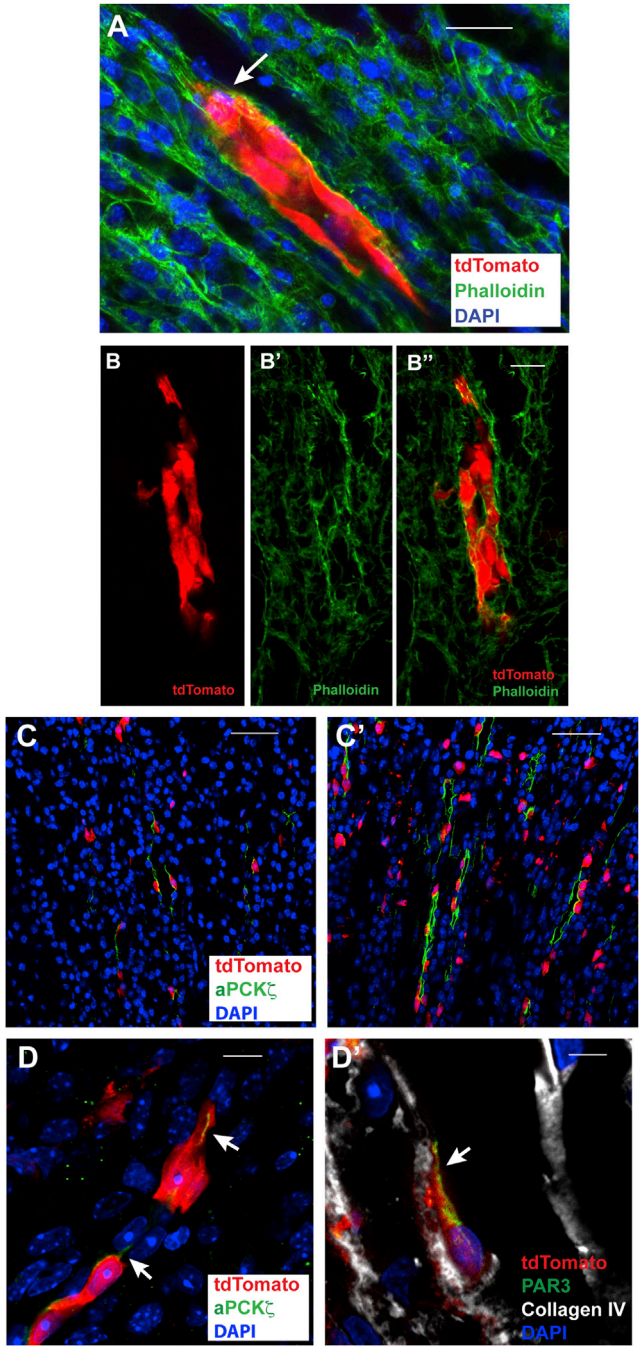

Figure 6. Expression of Polarity Proteins in *Zfyve27-CreERT2*-Marked Cells during Kidney Repair

(A) Groups of *Zfyve27-CreERT2*-marked cells with actin polymerization in the leading cells (arrow) 8 days after KI, performed 10 days pTM. Scale bar, 20 μm.

(B–B″) Group of *Zfyve27-CreERT2*-marked cells with actin polymerization at the edges of the cell cluster 8 days after KI. Scale bar, 50 μm.

(C and C′) aPKCζ expression in the upper papilla of the control (C) and injured (C′) kidneys 3 days after KI, performed 10 days pTM. Scale bar, 60 μm.

(D and D′) High-power confocal microphotographs of *Zfyve27-CreERT2*-marked cells 3 days after KI, performed 10 days pTM, expressing aPKCζ (arrows in D; scale bar, 20 μm) and PAR3 (arrow in D′; scale bar, 20 μm) at their leading processes.

membrane implies that these cells initially located in the interstitial might begin to populate injured medullary tubules.

Another striking change induced by KI was the appearance of aggregated clusters of *Zfyve27-CreERT2*-marked cells that exhibited actin polymerization either in the leading cells (Figure 6A) or at the edges of the cell cluster (Figures 6B–6B″), suggesting collective cell migration (Lucas et al., 2013; Xu et al., 2014), a process originally discovered during gastrulation but subsequently found in a variety of adult systems including mammary gland morphogenesis and epithelial organ repair (Friedl and Gilmour, 2009), including zebrafish kidney (Palmyre et al., 2014).

Finally, migrating epithelial cells become polarized, exhibiting an apical complex of aPKCζ, PAR3, and PAR6, proteins which accumulate in the leading edges of cellular projections during cell migration (Shin et al., 2007). We found that 3 days after KI, aPKCζ expression markedly increased in the papilla of the injured kidney (Figures 6C and 6C′). In addition, high-power confocal microscopy showed that expression of aPKCζ (Figure 6D) and PAR3 was concentrated at the leading processes of tdTomato$^+$ elongated cells (Figure 6D′). In non-injured kidney aPKCζ was restricted to few *Zfyve27-CreERT2*-marked cells in the papilla. It is interesting to note that protrudin/*Zfyve27* has been associated with development of large protrusions in neurons and contains FYVE domains that bind phosphatidylinositol 3-phosphate molecules (Raiborg et al., 2015) similarly to CDC42, another FYVE domain-containing protein that is involved in polarized motility.

These studies demonstrate that after injury the *Zfyve27-Cre*-marked cells change shape, display cellular projections that invade extracellular matrix, aggregate, and become polarized, all consistent with cell migration, including collective cell migration as seen in other organs during response to injury. While it is likely that the new tubules containing tdTomato$^+$ cells after kidney repair derive from the epithelial protrudin-expressing cells, these results raise the possibility that interstitial progenitor cells might invade the tubule and proliferate, replacing tubular epithelial cells. Indeed, integration of interstitial cells into nephron epithelia has previously been reported (Li et al., 2015), although more direct studies will be needed before this issue can be settled.

Migratory Capacity of *Zfyve27-CreERT2*-Marked Cells

As direct demonstration of cell migration in mammalian kidney in vivo is currently not possible, to test whether

Zfyve27-CreERT2-marked cells in the upper papilla had migratory capacity, we examined their behavior during organ culture. One half of a kidney from *Zfyve27-CreERT2*; *R*-tdTomato mice was analyzed with a two-photon microscope whereby the tdTomato$^+$ cells in the upper papilla were easily identified and the fluorescein isothiocyanate (FITC)-labeled papilla provided spatial information (see Figure S4A). In three different experiments, 233 *Zfyve27-CreERT2*-marked cells were detected, and 28 of these cells (12%) were found to be moving with an average speed of 46.6 ± 4.0 μm/h (mean ± SE). In one experiment, two tdTomato$^+$ had velocities greater than 100 μm/h and, suspected of being circulating cells, were excluded from the analysis. Interestingly, almost three-fourths of the 28 moving cells were migrating away from the FITC-containing lower papilla and toward the medulla. An experiment is shown in the movie of Figure S4B.

DISCUSSION

The adult kidney has a low rate of homeostatic cell cycling; yet, following injury, even one severe enough to cause total renal failure, widespread cell proliferation and functional recovery can occur. The mechanisms responsible for generation of new kidney cells during homeostasis and during organ repair remain poorly understood. Our previous studies had suggested that pLRCs might function to replenish these damaged cells, but we sought to find a lineage marker to allow definitive tracing of the progeny of these cells. Here we found that *Zfyve27* (protrudin) is a marker of a subpopulation of the pLRCs and using *Zfyve27-CreERT2* lines, we found that marked cells were most abundant in the upper part of the kidney papilla but that other parts of the kidney also had cells, albeit at much lower numbers. These labeled (and protrudin-expressing) cells were themselves label-retaining and cycled at much lower rates than the rest of the renal cells. Remarkably, they did not seem to participate in cell replacement during homeostasis or even kidney repair after modest injury. Yet, during severe KI these cells generated clones that populated large segments of injured tubules and, even more surprisingly, these tubules seemed to be located specifically in the kidney medulla rather than the cortex. Following severe injury, these cells continued to cycle longer than the rest of the kidney, explaining perhaps the extensive replacement of medullary tubules by their progeny. Hence, these results demonstrate that in the kidney (as in other epithelial organs) there exist multiple pools of progenitor cells, each of which is responsible for specific and perhaps anatomically distinct roles.

We identified the *Zfyve27* marker based on isolation of pLRCs that expressed the chimeric protein H2B-GFP. This protein has been found to be retained for a long time by cells that do not or seldom cycle and to dilute into the progeny of dividing cells (Brennand et al., 2007; Wilson et al., 2008; Foudi et al., 2009). Although these studies strongly suggested that H2B-GFP retention is a good marker for low-cycling cells, it is still theoretically possible that in the kidney papilla H2B-GFP is degraded at variable rates in different cells and that "H2B-GFP retention" is unrelated to cycling activity. However, in our previous studies we had found that the H2B-GFP-retaining cells of the kidney had the same location as those that retained BrdU, and they responded to injury in a qualitatively and quantitatively similar manner (Oliver et al., 2004, 2009).

The *Zfyve27*-marked cells in the papilla, as well as many other papillary cells (see Table S3), contain cell-surface markers found in a population of scattered proximal tubular cells (Smeets et al., 2013) implicated in kidney regeneration. However, because *Zfyve27*-marked cells in the cortex and medulla were very sparse, our flow cytometry analysis was restricted to papillary cells, and it is unknown whether cortical and medullary cells contain the same markers and are related to those in the papilla.

We had previously shown that after KI pLRCs migrated out of the upper papilla, and we show here that *Zfyve27-CreERT2*-marked cells assume a phenotype compatible with migratory behavior, even collective cell migration extending protrusions and filopodia in a polarized manner. Indeed, in ex vivo organ culture these marked cells were capable of moving at considerable speeds. Protrudin was initially identified as important in endocytosis, and it is well known that endocytosis is a critical mechanism in the formation of the leading edge during polarized motility (Bretscher, 2014). Moreover, recent studies have shown that protrudin (in neurons) binds to motor proteins, facilitating the movement of membrane to the surface to induce membrane extensions (Raiborg et al., 2015). While final proof of cell migration during repair of mammalian kidney in vivo would require additional studies with more invasive methods, we suggest that the *Zfyve27*-marked cells were identified (serendipitously) as those pLRCs that migrate in response to injury.

Generation of new cells during kidney repair has long been assumed to result from proliferation of surviving terminally differentiated cells. However, much of the modern evidence has used lineage tracing such as *Six2* (Humphreys et al., 2008) or a terminally differentiated marker (such as the proximal tubule phosphate transporter) (Kusaba et al., 2014). Such studies cannot eliminate the possibility that nephron segments might contain progenitor cells that express these markers or are derived from this lineage. Indeed, we found that some *Six2*-derived cells in the papilla expressed protrudin, as were some pLRCs, and together with *Zfyve27*-marked cells, protrudin-expressing cells (as well as

pLRCs) were found in all three currently known embryonic cell lineages present in papilla: interstitial as well as the two epithelial cells (*Six2*-derived and collecting ducts). Thus, each different pool of pLRCs (or *Zfyve27*-marked) cells might generate progeny restricted to their parent compartment; therefore the new tubules containing tdTomato$^+$ cells found after kidney repair most likely derive from the epithelial protrudin-expressing cells.

This finding is compatible with results showing that during kidney repair *Six2*-marked cells showed no dilution of the marker after kidney regeneration (Humphreys et al., 2008). Moreover, recent studies by Rinkevich et al. (2014) using the actin promoter to generate random single-cell clones in the adult kidney showed that some marked cells with high proliferation capacity expanded and generated tracing events restricted to specific nephron segments, indicating that the adult kidney likely contains precursor cells that are segment specific. They also found that cells with high proliferation capacity were Wnt responsive, raising the question of whether the *Zfyve27-CreERT2*-labeled cells (likewise with high proliferative capacity after KI) might be the same population as the Wnt-responsive cells identified by Rinkevich et al. (2014), a line of inquiry that we plan to pursue in the future.

The full power of the *Zfyve27-CreERT2*-marked cells to regenerate tubules was observed only after severe KI, since milder injury known to induce apoptosis did not induce the cells to proliferate and there was only modest proliferation by the cells after 30 min of kidney ischemia, a potent stimulus for widespread cell cycling in the kidney (Forbes et al., 2000; Oliver et al., 2009). It is thus possible that recovery from modest injury depends on proliferation of another pool of progenitor cells that belongs to a different lineage. These might include the aforementioned segment-specific or other types of progenitors or even terminally differentiated cells, as occurs in the liver (Yanger et al., 2014). Severe injury might deplete these latter pools of progenitors, as was found elsewhere (Tian et al., 2011; Vaughan et al., 2015). The medullary restriction of the *Zfyve27-CreERT2*-labeled cells emphasizes that the kidney, like other organs (Page et al., 2013; Donati and Watt, 2015), appears to have several precursor cell populations to generate new cells. For instance, stem cells in different segments of an organ, such as the gut, possess cell-autonomous region specificity (Wang et al., 2015) and, while the vertebrate kidney is seen as an organ, it is made up of semi-autonomous units called nephrons (containing different cellular regions), which in more ancient animals are fully individual organs (Hazelton et al., 1988; Scimone et al., 2011).

Characterization of the *Zfyve27-CreERT2*-marked cells in the kidney remains to be completed, but work in other organs suggests several possibilities. They could be bona fide precursor/stem cells that in addition to multilineage potential are able to self-renew and are solely activated during severe organ injury, but to prove multipotency and self-renewal will require analysis of individual cells inside their niche in vivo. Another possibility could be that if the kidney papilla is, as we previously suggested (Oliver et al., 2004), a precursor/stem cell niche, severe injury might have ablated resident stem cells and signals from the niche would then induce *Zfyve27-CreERT2*-marked (and other) cells to repopulate the niche and, by changing cell identity, become facultative stem cells, as found in regeneration of several organs (Tian et al., 2011; van Es et al., 2012).

EXPERIMENTAL PROCEDURES

Genome Expression Analysis of pLRCs

All animal experiments were performed under the oversight of the Institutional Animal Care and Use Committee of Columbia University.

To obtain the transcription profile of the pLRCs, we pulsed H2B-GFP mice with doxycycline during embryonic life and chased to ~2–3 months, as described by Oliver et al. (2009). In five different experiments, nine mice were euthanized and the kidney papillae isolated. Papillary cells were dispersed with collagenase digestion as described by Oliver et al. (2009). To label cells of bone marrow and endothelia origin, we briefly incubated cells with anti-mouse antibodies to CD45, TER119, and CD31, all coupled to PE (Becton Dickinson). In a BD FACSria, PE-negative live cells (DAPI-negative) were sorted into GFP-positive and GFP-negative (~2,000 cells in each sample) populations directly into lysis buffer. After RNA extraction and labeling, samples were analyzed with Two-Color Agilent Whole Mouse Genome Microarrays (Miltenyi Biotec).

Generation of Mice to Label *Zfyve27*-Expressing Cells

To genetically mark, in a regulated manner, *Zfyve27*-expressing cells, we first inserted a CreERT2 cassette into the promoter of *Zfyve27*, and cloned an Frt-NEO-Frt (FNF) cassette downstream of the CreERT2 to amplify the CreERT2-FNF cassette by high-fidelity PCR (Invitrogen AccuPrime High-Fidelity Taq PCR kit) with primers harboring 50-bp short homologies from both sides of the *Zfyve27* ATG codon. This CreERT2-FNF cassette was then recombined into the *Zfyve27* ATG codon of a BAC-containing *Zfyve27* gene by BAC recombining method. A gene-targeting vector was then generated by retrieving a 2-kb short arm (5′ to CreERT2-FNF insertion), CreERT2-FNF, and a 5-kb long arm (CreERT2-FNF to 3′) onto a plasmid carrying diphtheria toxin α chain (DTA cassette) as negative selection during gene targeting. 10 μg of pMCS-*Zfyve27-CreERT2*-DTA was linearized by AscI and electroporated into KV1 embryonic stem cells, and selected with 200 μg/ml G418 for 6 days. G418-resistant colonies were picked and screened for homologous recombination by PCR. Targeted embryonic stem cell clones were injected into C57BL/6 blastocysts to generate chimeras. Male chimeras were bred to C57BL6 females to transmit the *Zfyve27-CreERT2* allele. *Neo* cassette was then removed by breeding to ACTB-Flpe deleter mice (Jackson Laboratories; stock

number 019100). Mice colonies were maintained in C57BL6. For genotyping, the following primers were used: forward: GGCCTCATGAAGAGTGATAGGCTTT; reverse: TAATGCAGGCA AATTTTGGTGTACG.

Statistical Analysis

Data are shown as mean ± SEM and were analyzed by Student's t test or, when appropriate, ANOVA with Bonferroni correction for multiple comparisons. Where appropriate for transformed values, the Tukey-Kramer multiple comparison test was used (Zar, 1984).

SUPPLEMENTAL INFORMATION

Supplemental Information includes Supplemental Experimental Procedures, four figures, five tables, and one movie and can be found with this article online at http://dx.doi.org/10.1016/j.stemcr.2016.03.008.

AUTHOR CONTRIBUTIONS

J.A.O. and R.V.S. designed and performed the experiments and discussed the results. S.J. performed experiments, discussed the results, performed the confocal imaging and organ culture assay, and maintained the mouse lines. Q.-Y.Z., A.D., and W.W. performed experiments and discussed the results. T.H. designed and performed experiments and discussed the results. Q.A. designed experiments and discussed the results. J.A.O. and Q.A. wrote the manuscript.

ACKNOWLEDGMENTS

The authors thank Chyuan-Sheng Lin from the Transgenic Mouse Facility at the Herbert Irving Comprehensive Cancer Center at Columbia University for development of the *Zfyve27-CreERT2* mice; Theresa Swayne from the Confocal and Specialized Microscopy Shared Resource of the Herbert Irving Comprehensive Cancer Center at Columbia University for support for the confocal imaging and 2-photon microscopy (she is supported by NIH grant #P30 CA013696, National Cancer Institute, and the Nikon A1RMP confocal microscope was purchased with NIH grant #S10 RR025686); Kristie Gordon from the Flow Cytometry Shared Resource Facility of the Herbert Irving Comprehensive Cancer Center at Columbia University for support with FCAS; Mathew Zimmer from the New York State Foundation for support with flow cytometry; and Roseann Zott and Serge Cremers from the Irving Institute for Clinical and Translational Research for the LC/MS measurements.

Received: August 3, 2015
Revised: March 22, 2016
Accepted: March 23, 2016
Published: April 21, 2016

REFERENCES

Appel, D., Kershaw, D.B., Smeets, B., Yuan, G., Fuss, A., Frye, B., Elger, M., Kriz, W., Floege, J., and Moeller, M.J. (2009). Recruitment of podocytes from glomerular parietal epithelial cells. J. Am. Soc. Nephrol. *20*, 333–343.

Barker, N., van Es, J.H., Kuipers, J., Kujala, P., van den Born, M., Cozijnsen, M., Haegebarth, A., Korving, J., Begthel, H., Peters, P.J., et al. (2007). Identification of stem cells in small intestine and colon by marker gene Lgr5. Nature *449*, 1003–1007.

Berger, K., Bangen, J.M., Hammerich, L., Liedtke, C., Floege, J., Smeets, B., and Moeller, M.J. (2014). Origin of regenerating tubular cells after acute kidney injury. Proc. Natl. Acad. Sci. USA *111*, 1533–1538.

Blikslager, A.T., Moeser, A.J., Gookin, J.L., Jones, S.L., and Odle, J. (2007). Restoration of barrier function in injured intestinal mucosa. Physiol. Rev. *87*, 545–564.

Brennand, K., Huangfu, D., and Melton, D. (2007). All beta cells contribute equally to islet growth and maintenance. PLoS Biol. *5*, e163.

Bretscher, M.S. (2014). Asymmetry of single cells and where that leads. Annu. Rev. Biochem. *83*, 275–289.

Chen, C.C., Wang, L., Plikus, M.V., Jiang, T.X., Murray, P.J., Ramos, R., Guerrero-Juarez, C.F., Hughes, M.W., Lee, O.K., Shi, S., et al. (2015). Organ-level quorum sensing directs regeneration in hair stem cell populations. Cell *161*, 277–290.

Donati, G., and Watt, F.M. (2015). Stem cell heterogeneity and plasticity in epithelia. Cell Stem Cell *16*, 465–476.

Forbes, J.M., Hewitson, T.D., Becker, G.J., and Jones, C.L. (2000). Ischemic acute renal failure: long-term histology of cell and matrix changes in the rat. Kidney Int. *57*, 2375–2385.

Foudi, A., Hochedlinger, K., Van Buren, D., Schindler, J.W., Jaenisch, R., Carey, V., and Hock, H. (2009). Analysis of histone 2B-GFP retention reveals slowly cycling hematopoietic stem cells. Nat. Biotechnol. *27*, 84–90.

Friedl, P., and Gilmour, D. (2009). Collective cell migration in morphogenesis, regeneration and cancer. Nat. Rev. Mol. Cell Biol. *10*, 445–457.

Hazelton, S.R., Parker, S.W., and Spring, J.H. (1988). Excretion in the house cricket (*Acheta domesticus*): fine structure of the Malpighian tubules. Tissue Cell *20*, 443–460.

Humphreys, B.D., Valerius, M.T., Kobayashi, A., Mugford, J.W., Soeung, S., Duffield, J.S., McMahon, A.P., and Bonventre, J.V. (2008). Intrinsic epithelial cells repair the kidney after injury. Cell Stem Cell *2*, 284–291.

Ito, M., Yang, Z., Andl, T., Cui, C., Kim, N., Millar, S.E., and Cotsarelis, G. (2007). Wnt-dependent de novo hair follicle regeneration in adult mouse skin after wounding. Nature *447*, 316–320.

Kumar, S., Liu, J., Pang, P., Krautzberger, A.M., Reginensi, A., Akiyama, H., Schedl, A., Humphreys, B.D., and McMahon, A.P. (2015). Sox9 activation highlights a cellular pathway of renal repair in the acutely injured mammalian kidney. Cell Rep. *12*, 1325–1338.

Kusaba, T., Lalli, M., Kramann, R., Kobayashi, A., and Humphreys, B.D. (2014). Differentiated kidney epithelial cells repair injured proximal tubule. Proc. Natl. Acad. Sci. USA *111*, 1527–1532.

Li, J., Ariunbold, U., Suhaimi, N., Sunn, N., Guo, J., McMahon, J.A., McMahon, A.P., and Little, M. (2015). Collecting duct-derived cells display mesenchymal stem cell properties and retain selective in vitro and in vivo epithelial capacity. J. Am. Soc. Nephrol. *26*, 81–94.

Lucas, E.P., Khanal, I., Gaspar, P., Fletcher, G.C., Polesello, C., Tapon, N., and Thompson, B.J. (2013). The Hippo pathway polarizes

the actin cytoskeleton during collective migration of *Drosophila* border cells. J. Cell Biol. *201*, 875–885.

Mascré, G., Dekoninck, S., Drogat, B., Youssef, K.K., Broheé, S., Sotiropoulou, P.A., Simons, B.D., and Blanpain, C. (2012). Distinct contribution of stem and progenitor cells to epidermal maintenance. Nature *489*, 257–262.

Matsuzaki, F., Shirane, M., Matsumoto, M., and Nakayama, K.I. (2011). Protrudin serves as an adaptor molecule that connects KIF5 and its cargoes in vesicular transport during process formation. Mol. Biol. Cell. *22*, 4602–4620.

Oliver, J.A., Maarouf, O., Cheema, F.H., Martens, T.P., and Al-Awqati, Q. (2004). The renal papilla is a niche for adult kidney stem cells. J. Clin. Invest. *14*, 795–804.

Oliver, J.A., Klinakis, A., Cheema, F.H., Friedlander, J., Sampogna, R.V., Martens, T.P., Liu, C., Efstratiadis, A., and Al-Awqati, Q. (2009). Proliferation and migration of label-retaining cells of the kidney papilla. J. Am. Soc. Nephrol. *20*, 2315–2327.

Page, M.E., Lombard, P., Ng, F., Göttgens, B., and Jensen, K.B. (2013). The epidermis comprises autonomous compartments maintained by distinct stem cell populations. Cell Stem Cell *13*, 471–482.

Palmyre, A., Lee, J., Ryklin, G., Camarata, T., Selig, M.K., Duchemin, A.L., Nowak, P., Arnaout, M.A., Drummond, I.A., and Vasilyev, A. (2014). Collective epithelial migration drives kidney repair after acute injury. PLoS One *9*, e101304.

Raiborg, C., Wenzel, E.M., Pedersen, N.M., Olsvik, H., Schink, K.O., Schultz, S.W., Vietri, M., Nisi, V., Bucci, C., Brech, A., et al. (2015). Repeated ER-endosome contacts promote endosome translocation and neurite outgrowth. Nature *520*, 234–238.

Ridley, A.J., Schwartz, M.A., Burridge, K., Firtel, R.A., Ginsberg, M.H., Borisy, G., Parsons, J.T., and Horwitz, A.R. (2003). Cell migration: integrating signals from front to back. Science *302*, 1704–1709.

Rinkevich, Y., Montoro, D.T., Contreras-Trujillo, H., Harari-Steinberg, O., Newman, A.M., Tsai, J.M., Lim, X., Van-Amerongen, R., Bowman, A., Januszyk, M., et al. (2014). In vivo clonal analysis reveals lineage-restricted progenitor characteristics in mammalian kidney development, maintenance, and regeneration. Cell Rep. *7*, 1270–1283.

Rock, J.R., Onaitis, M.W., Rawlins, E.L., Lu, Y., Clark, C.P., Xue, Y., Randell, S.H., and Hogan, B.L. (2009). Basal cells as stem cells of the mouse trachea and human airway epithelium. Proc. Natl. Acad. Sci. USA *106*, 12771–12775.

Romagnani, P., Rinkevich, Y., and Dekel, B. (2015). The use of lineage tracing to study kidney injury and regeneration. Nat. Rev. Nephrol. *11*, 420–431.

Ronconi, E., Sagrinati, C., Angelotti, M.L., Lazzeri, E., Mazzinghi, B., Ballerini, L., Parente, E., Becherucci, F., Gacci, M., Carini, M., et al. (2009). Regeneration of glomerular podocytes by human renal progenitors. J. Am. Soc. Nephrol. *20*, 322–332.

Scimone, M.L., Srivastava, M., Bell, G.W., and Reddien, P.W. (2011). A regulatory program for excretory system regeneration in planarians. Development *138*, 4387–4398.

Shin, K., Wang, Q., and Margolis, B. (2007). PATJ regulates directional migration of mammalian epithelial cells. EMBO Rep. *8*, 158–164.

Singh, S.R., Liu, W., and Hou, S.X. (2007). The adult *Drosophila* malpighian tubules are maintained by multipotent stem cells. Cell Stem Cell *1*, 191–203.

Shirane, M., and Nakayama, K.I. (2006). Protrudin induces neurite formation by directional membrane trafficking. Science *314*, 818–821.

Smeets, B., Boor, P., Dijkman, H., Sharma, S.V., Jirak, P., Mooren, F., Berger, K., Bornemann, J., Gelman, I.H., Floege, J., et al. (2013). Proximal tubular cells contain a phenotypically distinct, scattered cell population involved in tubular regeneration. J. Pathol. *229*, 645–659.

Sun, J., Ramos, A., Chapman, B., Johnnidis, J.B., Le, L., Ho, Y.J., Klein, A., Hofmann, O., and Camargo, F.D. (2014). Clonal dynamics of native haematopoiesis. Nature *514*, 322–327.

Tarlow, B.D., Pelz, C., Naugler, W.E., Wakefield, L., Wilson, E.M., Finegold, M.J., and Grompe, M. (2014). Bipotential adult liver progenitors are derived from chronically injured mature hepatocytes. Cell Stem Cell *15*, 605–618.

Tian, H., Biehs, B., Warming, S., Leong, K.G., Rangell, L., Klein, O.D., and de Sauvage, F.J. (2011). A reserve stem cell population in small intestine renders Lgr5-positive cells dispensable. Nature *478*, 255–259.

van Es, J.H., Sato, T., van de Wetering, M., Lyubimova, A., Nee, A.N., Gregorieff, A., Sasaki, N., Zeinstra, L., van den Born, M., Korving, J., et al. (2012). Dll1+ secretory progenitor cells revert to stem cells upon crypt damage. Nat. Cell Biol. *14*, 1099–1104.

Vaughan, A.E., Brumwell, A.N., Xi, Y., Gotts, J.E., Brownfield, D.G., Treutlein, B., Tan, K., Tan, V., Liu, F.C., Looney, M.R., et al. (2015). Lineage-negative progenitors mobilize to regenerate lung epithelium after major injury. Nature *517*, 621–625.

Veniaminova, N.A., Vagnozzi, A.N., Kopinke, D., Do, T.T., Murtaugh, L.C., Maillard, I., Dlugosz, A.A., Reiter, J.F., and Wong, S.Y. (2013). Keratin 79 identifies a novel population of migratory epithelial cells that initiates hair canal morphogenesis and regeneration. Development *140*, 4870–4880.

Wang, X., Yamamoto, Y., Wilson, L.H., Zhang, T., Howitt, B.E., Farrow, M.A., Kern, F., Ning, G., Hong, Y., Khor, C.C., et al. (2015). Cloning and variation of ground state intestinal stem cells. Nature *522*, 173–178.

Wilson, A., Laurenti, E., Oser, G., van der Wath, R.C., Blanco-Bose, W., Jaworski, M., Offner, S., Dunant, C.F., Eshkind, L., Bockamp, E., et al. (2008). Hematopoietic stem cells reversibly switch from dormancy to self-renewal during homeostasis and repair. Cell *135*, 1118–1129.

Xu, H., Ye, D., Behra, M., Burgess, S., Chen, S., and Lin, F. (2014). Gβ1 controls collective cell migration by regulating the protrusive activity of leader cells in the posterior lateral line primordium. Dev. Biol. *385*, 316–327.

Yanger, K., Knigin, D., Zong, Y., Maggs, L., Gu, G., Akiyama, H., Pikarsky, E., and Stanger, B.Z. (2014). Adult hepatocytes are generated by self-duplication rather than stem cell differentiation. Cell Stem Cell *15*, 340–349.

Zar, J.H. (1984). Biostatistical Analysis, Second Edition (Prentice-Hall), 239–241.

Stem Cell Reports, Volume *6*

Supplemental Information

A Subpopulation of Label-Retaining Cells of the Kidney Papilla Regenerates Injured Kidney Medullary Tubules

Juan A. Oliver, Rosemary V. Sampogna, Sumreen Jalal, Qing-Yin Zhang, Alexander Dahan, Weiwei Wang, Tian Huai Shen, and Qais Al-Awqati

Figure Sn 1

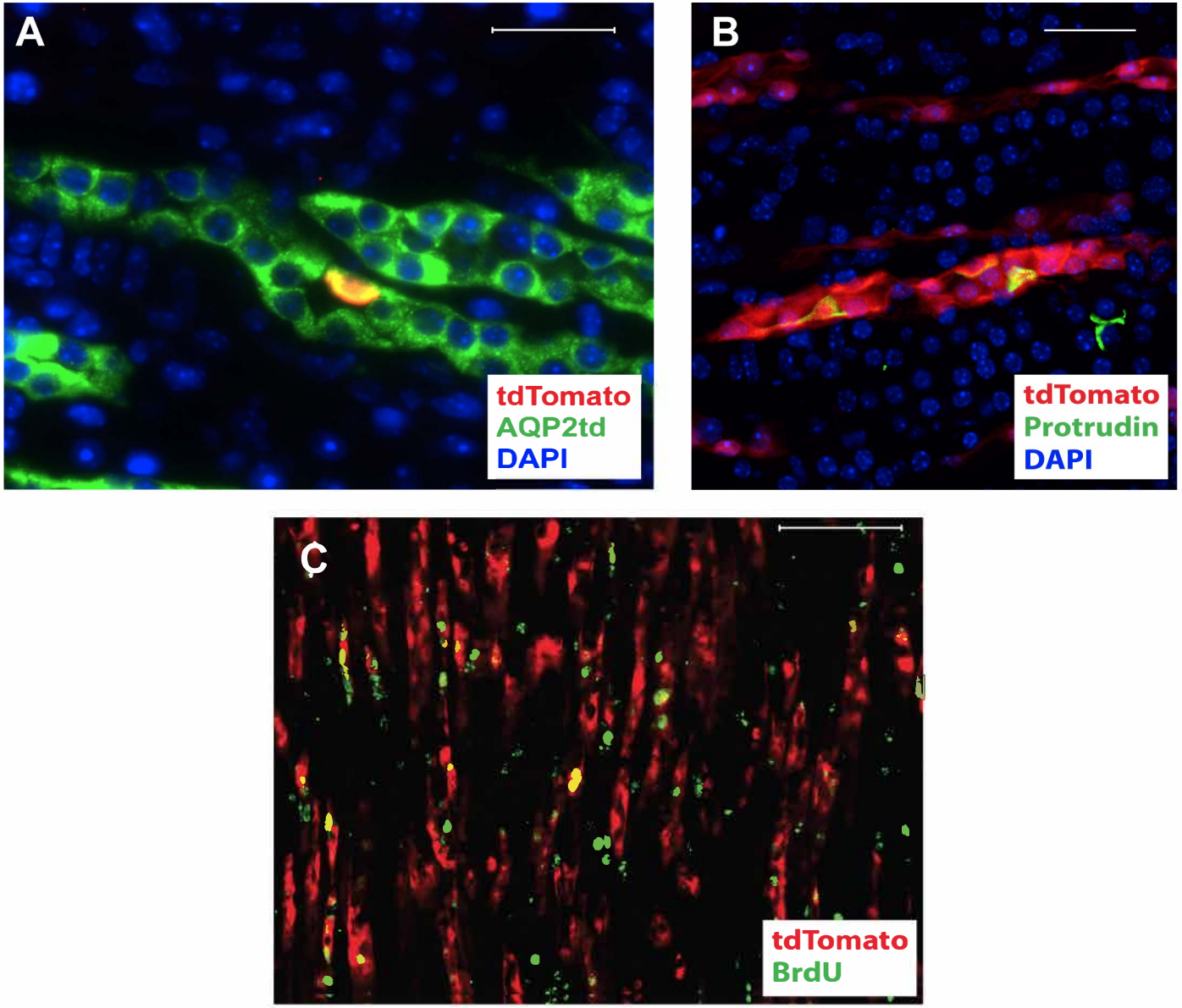
A
tdTomato
AQP2td
DAPI
B
tdTomato
Protrudin
DAPI
C
tdTomato
BrdU

Figure Sn 2

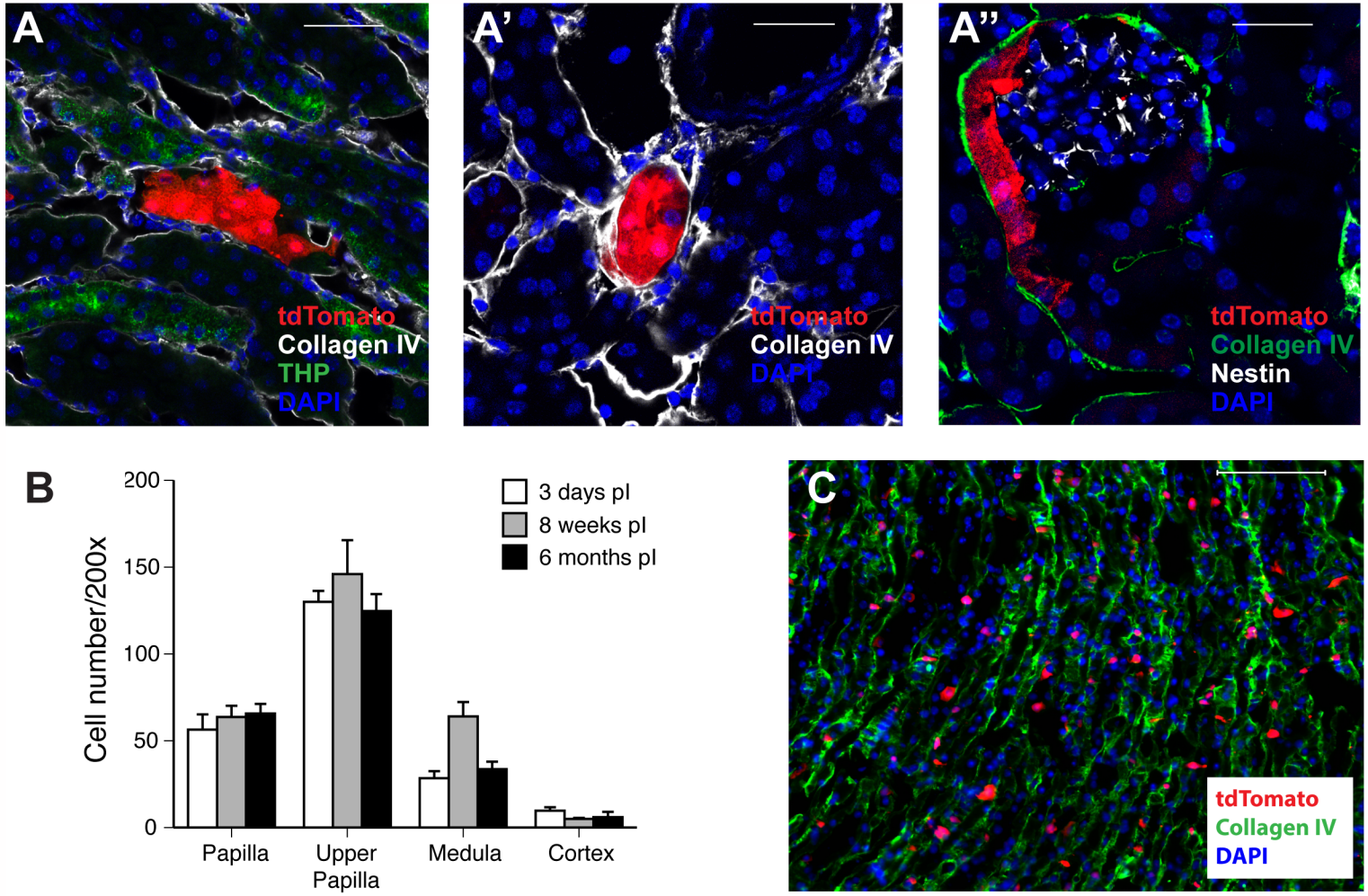
A
tdTomato
Collagen IV
THP
DAPI
A'
tdTomato
Collagen IV
DAPI
A''
tdTomato
Collagen IV
Nestin
DAPI
B
Cell number/200x
200
150
100
50
0
3 days pI
8 weeks pI
6 months pI
Papilla
Upper Papilla
Medula
Cortex
C
tdTomato
Collagen IV
DAPI

Figure Sn 3

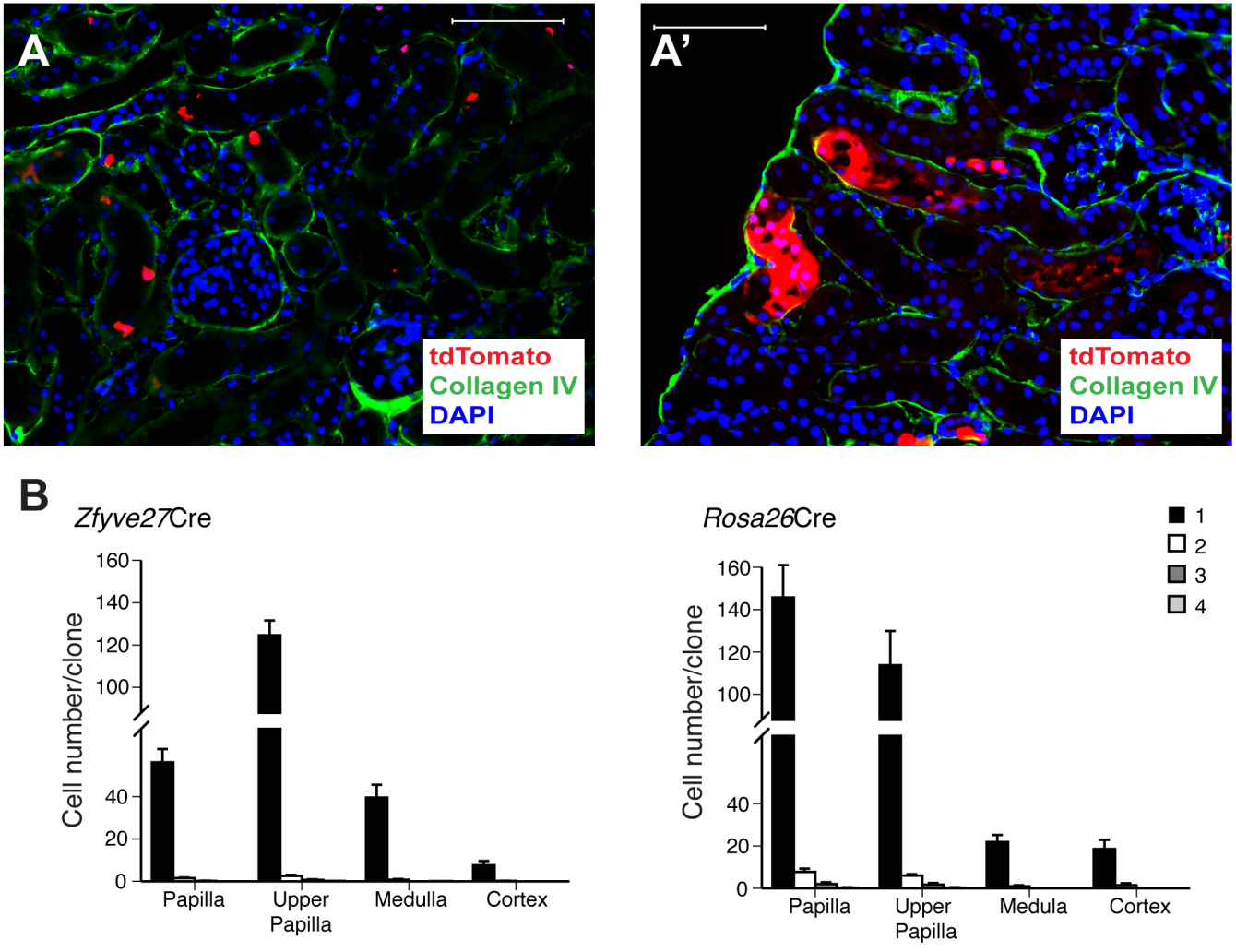
A
tdTomato
Collagen IV
DAPI
A'
tdTomato
Collagen IV
DAPI
B
Zfyve27Cre
Cell number/clone
160
140
120
100
40
20
0
Papilla
Upper Papilla
Medulla
Cortex
Rosa26Cre
1
2
3
4
Cell number/clone
160
140
120
100
40
20
0
Papilla
Upper Papilla
Medula
Cortex

Figure Sn 4

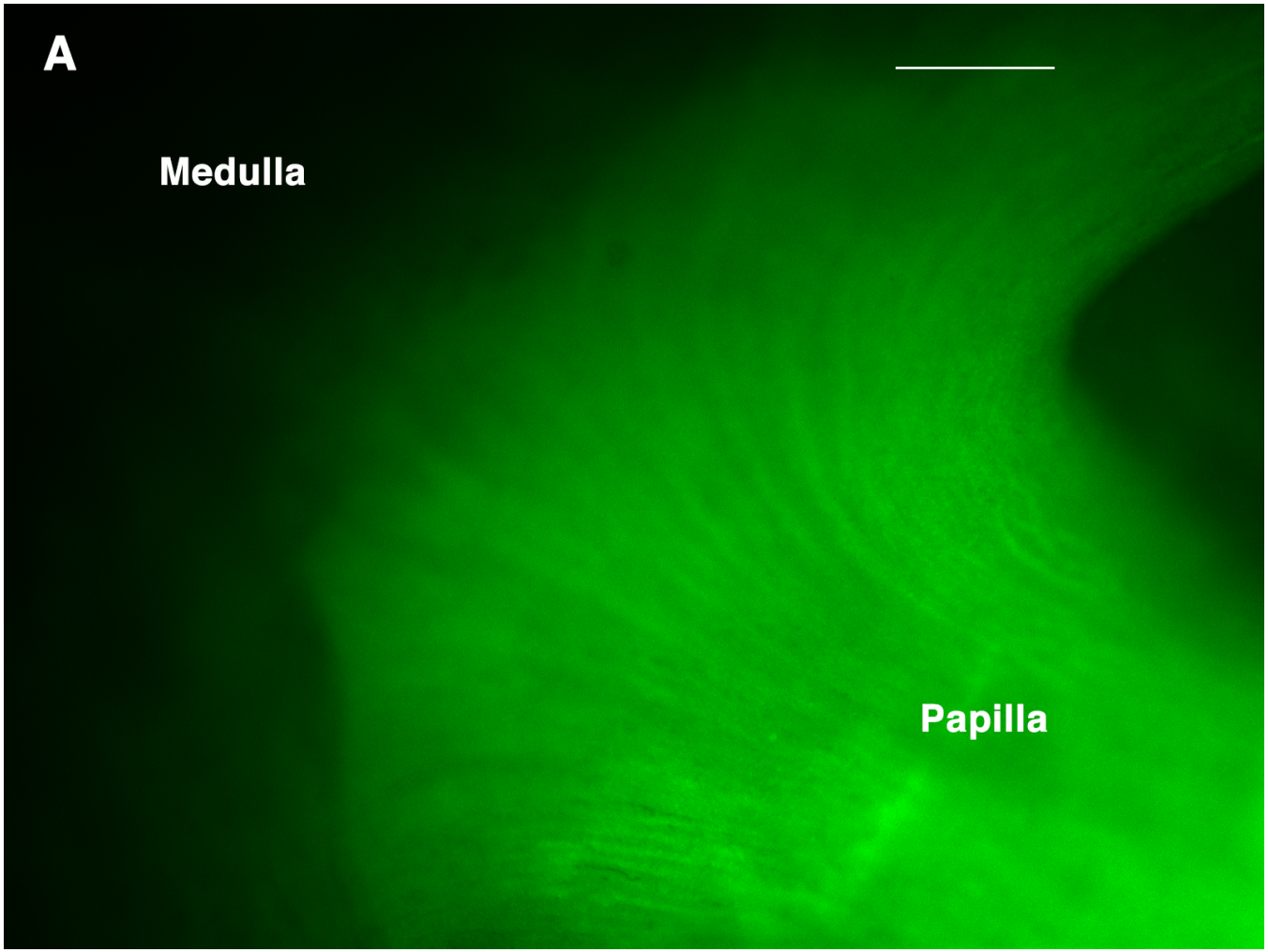

SUPPLEMENTAL FIGURE LEGENDS

Figure S1. A. *Zfyve27*-Cre*ERT2*-marked cells. 25% of *Zfyve27*-Cre*ERT2*-marked cells in the papilla were in collecting ducts (n=5 mice); i.e., were positive for AQP2, as shown. 2 weeks pTM. Scale bar 25μm. **B. *Six2*-derived cells express protrudin**. 14% of *Six2*Cre-marked cells expressing tdTomato in the papilla expressed protruding (n=4 mice). Scale bar 25 μm**. C**. **Papillary *Six2*-derived cells are pLRCs.**. Kidney papilla of *Six2*Cre;*Rosa26*-tdTomato mouse given BrdU at 3 days of age and chased for 3 months. Note BrdU-retention in tdTomato marked cells (i.e., *Six2*-derived). n = 3 mice; scale bar 50 μm.

Figure S2. Tracing events by *Zfyve27*-Cre*ERT2*-marked cells in homeostasis. A, A', A''. Rare tracing events by *Zfyve27*-CreERT2-marked cells in mice > 5 months pTM. **A.** Tubular segment made of *Zfyve27-CreERT2*-marked cells in the medulla; THP, Tamm Horsfall Protein (Scale bar 40 μm). **A'**. Transverse cut of a tubular segment made of *Zfyve27-CreERT2*-marked cells in the kidney medulla. Scale bar 40 μm. A''. Bowman's capsule with multiple contiguous *Zfyve27*-CreERT2-marked cells; nestin staining identifies podocytes. Scale bar 40 μm. **B**. ***Zfyve27-CreERT2*-marked cells after 5 days at 3 days, 8 weeks and 6 months pTM**. The number of cells in all regions did not significantly increase from those at 3 days post tamoxifen; n=3 to 8 mice; Mean±SE. **C.** Upper papilla. As illustrated, *Zfyve27*CreERT2-marked cells in the upper papilla (8 days pTM) were, except for very rare exceptions, at clonal density. Scale bar 50 μm.

Figure S3. *Rosa26*-Cre*ERT2*T-marked cells. A. In *Rosa26-CreERT2;R*-tdTomato mice 8 days pTM (5 mg / Kg) marked cells were at clonal, or near clonal density. Scale bar 50 μm. **A'.** In these mice however, tamoxifen (even at 10x lower doses) occasionally marked groups of cells (8 days pTM). Scale bar 50 μm. **B. Clonal analysis of tdTomato$^+$ cells in the non-injured kidney of *Zfyve27-CreERT2;R*-tdTomato (n=5) and *Rosa26-CreERT2;R*-tdTomato (n=6) 16 days pTM**. As shown, in all

regions of the kidney, most of the *Zfyve27*CreERT2-marked cells were single clones (97 %; left). In the kidneys with *Rosa26-CreERT2*-marked cells, 92 % of the cells were single clones (right). Mean±SE. The number of clones in different kidney regions is shown in the Y-axis and the 1 to 4 keys indicate number of cells per clone.

Figure S4. Kidney organ culture and migration of *Zfyve27*CreERT2-marked cells **A.** Kidney medulla and papilla of a *Zfyve27-CreERT2;R*-tdTomato mouse administered FITC-Dextran 8 days pTM. FICT-Dextran 10 min before kidney isolation labeled the kidney papilla but not medulla allowing spatial information about the cell movement direction. Scale bar 250 μm. **B.** Migration of *Zfyve27*CreERT2-marked cells in the upper papilla. The upper papilla was analyzed with 27 cuts of 3 μm thickness captured every 5 min during 8.2 h. The movie shows the maximum intensity projection of the Z series.

Table S1. qPCR fold change of candidate genes normalized to GAPDH

Gene Symbol	Fold overexpression	Standard deviation (+/-)
Bst1	17.4	2.1
Clk1	15.6	2.0
Cxcr4	9.1	1.6
Dach1	9.3	2.2
Dlg1	12.8	2.1
Dlg5	16.4	2.3
Dlg7	7.0	1.3
Erap1	8.6	1.4
Esr1	18.9	4.1
Fancd2	9.9	1.6
Flot1	8.2	1.5
Foxg1	11.3	1.4
G3bp1	22.7	3.9
Hoxa9	14.5	2.7
Hoxb5	12.5	1.9
Ly6e	17.7	2.7
Malat1	16.8	2.6
Ogt	14.9	1.8
Pax2	7.2	1.1
Podn	19.3	3.0
Ryk	8.3	1.9
Sssca1	12.9	2.2
Sfrs1	15.4	2.4
Syne2	5.8	0.8
Tm2d3	15.3	2.2
Tsg101	15.1	1.8
Tspan3	13.4	1.8
Tspan6	10.6	1.9
Zfyve27	13.3	1.6
Zmpste24	12.4	1.2

Table S2. Detection of proteins encoded by candidate genes by immunofluorescence microscopy in the Kidney.

Gene	*Result*
NPD	Collecting system
SGCB	Non-specific
TSG101	Negative
ERAP1	Non-specific, glomerulus, tubules
FLOT1	Few in papilla and medulla
CLK1	Non-specific
SFRS1	Non-specific
HOXA9	No papillary staining
HOXB9	Negative
SF2	Negative
ESRA	Papilla, medulla, uro-epithelium
TSG101	Negative
OGT	Non-specific
DACH1	Nuclear, mainly in papilla
ZMPSTE24	Negative
LY6A/E	Non-specific
GP130	Uro-epithelial, tubules and glomerulus
LGR5	Negative
ZYVE27	Papilla only

Table S3. Fraction (%) of *Zyve27*-CreERT2-marked; i.e., tdTomato^{-} and tdTomato^{+} cells in kidney papilla that expressed cell surface by flow cytometry analysis.

	tdTomato ^{negative}	tdTomato ^{positive}
CD24	94	100
CD29 (β1 integrin)	54	86
CD49f (α6 integrin)	36	57
CD133	30	53
SCA-1	73	78
CXCR4	22	54
CXCR7	56	70
CXCR4 + CXCR77	13	43

All data points from 3-4 independent experiments and each experiment contained cells from 2 mice. Isotype-specific antibodies were used as controls.

Table S4. Clonal analysis of *Zfyve27*CreERT2-marked cells in the kidneys of *Zfyve27-CreERT2;R*-tdTomato mice after one dose of tamoxifen (40 mg / Kg).

Kidney region	Total Cell number	Single clones	Double clones	% Single clones
Cortex	60	60	0	100
Medulla	166	164	1	99
Upper papilla	816	806	4	99
Papilla	155	155	0	100

n=6 mice; data obtained from 3-21 days pTM.

Table S5. Concentrations of Tamoxifen (TM) and 4-Hydroxytamoxifen (4-HO-TM) in mouse kidney papilla and in the cortex plus medulla.

	TM			4HO-TM	
	Papilla	Cortex+Medulla		Papilla	Cortex+Medulla
Exp #1	406.2	901.9		64.6	140.0
Exp #2	280.0	1142.3		37.9	150.7
Average	343.1	1022.1		51.3	145.4

The *Rosa26*-CreERT*2;R*-tdTomato bi-transgenic mice had many marked cells in the kidney papilla after 5 mg/Kg TM (see Figure 3A). We tested whether papillary accumulation of TM and/or its most active metabolite 4-Hydroxytamoxifen could account for this observation by measuring their concentration by liquid chromatography–mass spectrometry**.** However, as shown in the table, the concentration of both compounds was markedly lower in the papilla than in the rest of the kidney and the reason why these mice had such abundance of tdTomato^{+} cells in the papilla is unclear. For each experiment, 5 mice were given 40 mg / Kg TM for 5 consecutive days and euthanized 3 days later.

SUPPLEMENTAL EXPERIMENTAL PROCEDURES

Genome expression analysis of papillary LRCs

Gene expression analysis of the pLRCs from the H2B-GFP mouse (GFP^+ vs GFP-negative papillary cells) found 6,400 significantly up-regulated or down-regulated genes (fold-change greater than 2 or lower than 2 and $p< 0.01$). Output data including gene lists with complete raw data sets have been deposited in (GEO ID: GSE71693). We narrowed the candidate gene list to include those with fold-change greater than or lower than 5. Of these potential candidates, manual extraction revealed that 216 of 2713 transcripts (8%) were consistently over-expressed in the papillary LRCs versus the GFP-negative cells. We confirmed the over-expression of 30 of the most highly over-expressed genes in the LRCs versus the GFP-negative cells by first using the MessageBOOSTER cDNA Synthesis Kit (Epicentre, Madison, Wisconsin) to amplify mRNA and then by performing qPCR. Experiments were run in triplicate and fold-expression changes are shown in Table S1.

Mice

Mice were maintained at the Columbia University Medical Center Institute of Comparative Medicine, in accordance with its guidelines and all experiments were performed with approval of the IRB of Columbia University. H2B-GFP mice were as described (Oliver et al., 2009). Briefly, to obtain a line where administration of doxycycline caused expression of the fusion protein histone2B-GFP we used the previously published TetO-H2BGFP line (Tumbar et al., 2004) but instead of crossing it with a line with a keratin5-tTA driver, we crossed it with a *Rosa26*-rtTA line (Yu et al., 2005). *Rosa26*-rtTA;teto-H2BGFP bi-transgenic offspring did not express GFP but doxycycline administration through drinking water resulted in expression of histone2B-GFP (Oliver et al., 2009). The fusion protein histone2B-GFP is stable for at least six months in post-mitotic cells (e.g., photoreceptors) and in cycling cells it dilutes into their progeny (Brennand et al, 2007).

All other mice were obtained from Jackson Laboratories, specifically: the reporter mouse line B6.Cg-*Gt(ROSA)26Sor*$^{tm14(CAG-tdTomato)Hze}$/J (Number: 007914), the universal Cre mouse line B6.129-*Gt(ROSA)26Sor*$^{tm1(cre/ERT2)Tyj}$/J (Number: 008463), the *Six2* Cre line STOCK Tg(Six2-EGFP/cre)1Amc/J (Number 009606) and C57BL/6J (Number: 000664). For all these mouse lines, genotyping was performed as recommended by Jackson Laboratories.

Tamoxifen administration

Tamoxifen (Sigma) was prepared as described (Metzeger & Chambon 2001) and administered by intra-peritoneal injection at 40 mg/Kg once, unless specified. To determine the duration of CreERT2 action in the kidney after tamoxifen, we administered tamoxifen to 15 *Zfyve27*-CreERT2;*R*-tdTomato mice and sacrificed 3 mice each at days 1, 2, 3, 4 and 5 pTM. Quantification of all tdTomato^{+} cells showed that there were abundant cells at 24 h pTM, that their numbers increased slightly at 2 and 3 days but remained unchanged between days 3, 4 and 5 days pTM.

EdU administration

For normal mice, was dissolved in PBS at 8 mg/ml. This solution was introduced into an Alzet osmotic mini-pump (Number 2002) and implanted subcutaneously to *Zfyve27*-CreERT2;R-tdTomato adult mice under general anesthesia. During pump implantation, the mice were given 100 µg of EdU by subcutaneous injection. The mini-pumps delivered 96 µg of EdU daily for two weeks, at which time the mice were sacrificed and their kidneys harvested. Mice subjected to renal artery occlusion in order to injury the kidney were given EdU (dissolved in PBS at 2 g/ml) as a subcutaneous injection of 50 µg/gr at 8 AM and 6 PM the day before and at 8 AM the day of sacrificed, which took place 6 h after the last EdU injection.

Ischemic kidney injury (KI)

KI was induced as previously described by clamping the left renal artery (Oliver et al., 2009) for the specified time periods. Most KI experiments were done at least one week pTM. In a few instances, we performed KI 3 or 4 days pTM since after 3 days we found no evidence of CreERT2 activation (see above). The time interval between TM administration and KI is specified in the legends of all described experiments and it is expressed as time pTM; i.e., post-tamoxifen.

Immuno-detection and confocal microscopy

Kidneys were isolated and processed as described (Oliver et al., 2009). Most kidney sections were of 5 μm but 10-15 μm sections were obtained for confocal analysis. BrdU (Life Technologies) detection was done as previously described (Oliver et al., 2004), except where indicated. EdU (Life Technologies) was detected following the manufacturer protocol**.** Fluorescence signals were detected with a fluorescence microscope and an RT Slider SPOT digital camera (Diagnostic Instruments) and with an Axiovert 100 laser-scanning confocal microscope (model LSM 410; Carl Zeiss).

BrdU-detection in kidneys with tdTomato$^+$ cells. Immuno-detection of BrdU in kidney sections requires their incubation with HCl for ~ 30 min to allow effective antibody penetration. This resulted in loss of the tdTomato signal and a series of experiments was carried out to develop a procedure that attained effective anti-BrdU antibody penetration but retained the tdTomato signal. We found that by first treating the kidney sections with Target Retrieval Solution (Dako), followed by only 10 min of HCl and standard neutralization with NaOH, anti BrdU antibody penetration was efficient and the tdTomato signal partially preserved (see Figure 1F).

Quantification of Zfyve27CreERT-marked cells. For each mouse, of 12 consecutive 5 μm sections containing a complete sagittal cut (and including the papilla) of one of the two kidneys, section numbers 1, 6 and 12 were selected for analysis after staining with DAPI and a collagen IV antibody. In the fluorescence microscope and guided by the image of the collagen IV staining (in FITC), from the cortex, medulla and upper papilla, three random fields were selected at 200x unless specified. For the

smaller main body of the papilla, only two fields were selected. After selection, a photograph with the Rhodamine filter was taken and the number of tdTomato$^+$ quantified.

Quantification of EdU positive cells. In mice with Zfyve27CreERT-marked cells and that received EdU, kidney sections were stained with DAPI and EdU visualized as instructed by the manufacturer (Life Technologies). Three non-contiguous sections were analyzed as described in Quantification of Zfyve27CreERT-marked cells above and the number of DAPI$^+$ and tdTomato negative cells and of the tdTomato$^+$ cells quantified. In these two populations the number of EdU positive nuclei was next obtained and expressed as percentage of the total cells.

Clonal analysis of Zfyve27CreERT-marked cells. For each mouse, all individual tdTomato$^+$ cells present in the cortex, medulla, upper papilla and papilla of a 5 μm section were identified by co-staining their nuclei with DAPI. Single clones were defined as a tdTomato$^+$ cell containing a single nucleus and not contiguous to any other tdTomato$^+$ cell. Double cell clones when two contiguous tdTomato$^+$ cells containing two nuclei stained with DAPI.

Quantification of new tubules made of tdTomato$^+$ cells. Both the un-injured (control) and injured kidneys of *Zfyve27*CreERT2;R-tdTomato and of ROSACreERT2;R-tdTomato mice were sagittal sectioned and the side containing the papilla was mounted for tissue sections. Twenty 5 μm sections containing a complete sagittal cut of the kidney were obtained and sections numbered 1, 10 and 20 were stained for collagen IV and examined under the fluorescent microscope. A tubule made up of tdTomato$^+$ cells was define as a group of these cells that made a circular tubular structure or > 10 tdTomato$^+$ longitudinally contiguous cells. For each kidney, all tubules present in a section were counted and averaged. Measurements of tubular length were done with ImageJ.

qPCR.

Was performed as described (Oliver et al., 2009).

Flow cytometry

Adult mice with Zfyve27CreERT-marked cells were sacrificed and the papillae of their kidneys isolated. After mincing and incubation with collagenase I (Worthington), papillary cells were isolated as described (Oliver 2004). Flow cytometry was carried as described (Oliver et al., 2009) except that given the intensity of the tdTomato signal, all antibodies (and appropriate isotype-specific controls) used were coupled to either APC or Alexa 647 and when an antibody couple to those fluors was not available, antibodies coupled to Pacific Blue were used.

Kidney organ culture and 2-photon microscopy

Because *Zfyve27* is also expressed in the bone marrow (see GeneAtlas U133A at http://biogps.org/#goto=genereport&id=118813) and given the kidney's extensive vascular network, we first determined how many of the *Zfyve27CreERT2*-marked cells in the kidney papilla were circulating cells originating in the bone marrow. To do this, we isolated papillary cell suspensions from *Zfyve27CreERT2*;*R*-tdTomato mice and probed them with a CD45-Alexa coupled antibody by flow cytometry. In three independent experiments, only 3.1 ± 0.2% (mean ± SE; n=6 mice) of all tdTomato$^+$ cells were also positive for CD45. Hence, a small fraction of the papillary tdTomato cells is of bone marrow origin.

Under general anesthesia, Zfyve27CreERT2;R-tdTomato mice previously treated with TM were given 5 mg of FITC-dextran (Life Technologies, D-1821) intravenously. After ~ 10 min, mice were sacrificed and one of their kidneys isolated. The FITC-dextran accumulated in the lower papilla (Lencer et al., 1990) and provided spatial orientation during microscopy (Figure S7). The kidney was sectioned by its sagittal plane so that the papilla was attached to only one kidney half. The sectioned surface of this half was then placed on a glass cover slide coated with Matrigel (BD Biosciences), covered with warmed DMEM containing 10% FCS and incubated for ~ 8 h at 37^{o}C in a 5% CO_2 atmosphere. After

incubation, the half kidney had attached to the Matrigel and was taken to the 2-photon microscope for analysis.

Kidneys were imaged by 2-photon excitation at 920 nm using a 25x/1.1 Apo-LWD water-immersion objective lens on a Nikon A1R MP multiphoton imaging system. Fluorescent proteins were detected with non-descanned detectors using standard green and red filters in the reflected light path. The culture dish was placed in a heated, humidified stagetop chamber with 5% CO_2 atmosphere. Cell movement was examined by obtaining serial 3 μm sections every 5 minutes for ~ 8 h while maintained the kidney in tissue culture conditions.

Antibodies

The antibodies used for immune-fluorescence were: AQP2, rabbit polyclonal (Sigma, A7310) and goat polyclonal (Abcam, ab105171); AQP1 rabbit polyclonal (Abcam; ab15080); BrdU, rat monoclonal (Abcam, ab6326); calbindin, rabbit polyclonal (Swant, CB38); CD11c rat monoclonal (clone M1/70, eBioscience, 14-0112-81); CD140b, rat monoclonal (clone APB5, eBioscience, 14-1402-81); CD146, rabbit monoclonal (Abcam, ab75769); CD68, rat monoclonal (Abcam, ab53444); CLC-K rabbit polyclonal (Santa Cruz, sc-292791), goat polyclonal (Santa Cruz, sc-21295) and rabbit polyclonal to CLC-K (Chemicon); collagen IV, rabbit polyclonal (Abcam, ab19808) and goat polyclonal (SouthernBiotech, 1340-01); megalin, goat polyclonal (Santa Cruz, sc-16478); p75NGFR, rabbit polyclonal (Abcam, ab38335); PAR3, rabbit polyclonal (Millipore; 07-330); perlecan, rat monoclonal A7L6 (Millipore, MAB1948P); PKC ζ, rabbit polyclonal (Santa Cruz; sc-216); protrudin, rabbit polyclonal (Santa Cruz, sc-102174) and rabbit polyclonal (Abbiotec, 252206); Sox9, rabbit polyclonal (Novus, NRP1-85551), Tamm Horsfall Protein sheep polyclonal (Chemicon, AB733). Nuclei were stained with DAPI (Invitrogen).

Antibodies used for flow cytometry were: APC rat anti-mouse CD45 (clone 30-F11, BioLegend) and V450 rat anti-mouse (BD, 560501); Alexa fluor 647 rat anti-mouse CD24 (clone M1/69, BioLegend, 101817); APC rat anti-mouse CD133 (clone 315-2C11, BioLegend, 141207); Alexa fluor 647 Armenian

hamster anti CD29 (clone HMβ1-1, BioLegend, 102213); Pacific Blue rat anti CD49f (clone GoH3, BioLegend, 313619); Alexa fluor 647 rat anti-mouse Ly-6A/E (Sca-1) (clone E13-161.7, BioLegend, 122517); Brilliant Viole 421 rat anti-mouse CD184 (clone 2B11/CXCR4, BD, 562738) and APC rat anti-mouse (clone 2B11, eBioscience, 17-9991-80); APC anti CXCR7 (clone 8F11-M16, BioLegend, 331113)

Reagents

Tamoxifen and 4-Hydroxytamoxifen were from Sigma; FITC-Dextran, 10,000 MW from Life Technologies (D-1821); EdU from Invitrogen (A10044); BrdU from Sigma (B9285) and Target Retrieval Solution from DAKO (S1699).

Liquid chromatography–mass spectrometry

Tissue samples were homogenized in water at a concentration of 1 mg/ml. Homogenates were extracted with 8 ml of hexane/methylene chloride: 3/2. Supernatants were evaporated under nitrogen and re-suspended in 50ul of 50 % methanol with 0.1 % formic acid. A Waters Acquity UPLC system with a 100 mm BEH C18 column was used for separation. The column was equilibrated with 75% water with 0.1% formic acid and 25% acetonitrile with 0.1% formic acid. A Waters XEVO TQS Tandem Mass Spectrometer was used for analyte detection. Our calibration curve was sensitive down to 25 pg /ml.

SUPPLEMENTAL REFERENCES

Brennand K, Huangfu D, Melton D. All beta cells contribute equally to islet growth and maintenance. PLoS Biol. 2007, 5: e163.

Lencer WI, Verkman AS, Arnaout MA, Ausiello DA, Brown D. Endocytic vesicles from renal papilla which retrieve the vasopressin-sensitive water channel do not contain a functional H+ ATPase. J Cell Biol. 1990; 111: 379-89.

Metzger D, Chambon P. Site- and time-specific gene targeting in the mouse. Methods. 2001; 24: 71-80.

Oliver JA, Klinakis A, Cheema FH, Friedlander J, Sampogna RV, Martens TP, Liu C, Efstratiadis A, Al-Awqati Q. Proliferation and migration of label-retaining cells of the kidney papilla. J Am Soc Nephrol. 2009; 20: 2315-27.

Tumbar T, Guasch G, Greco V, Blanpain C, Lowry WE, Rendl M, Fuchs E. Defining the epithelial stem cell niche in skin. Science 2004 Jan 16;303(5656):359-63.

Yu HM, Liu B, Chiu SY, Costantini F, Hsu W. Development of a unique system for spatiotemporal and lineage-specific gene expression in mice. Proc Natl Acad Sci U S A. 2005; 102: 8615-20.